

Design and Evaluation of Bivalent K-Ras Inhibitors That Target the CAAX Binding Site and the Acidic Surface of Farnesyltransferase and Geranylgeranyltransferase I

Naomi Horiuchi,^[a] Rania Omer,^[b] Fumitoshi Sugino,^[a] Nanami Ogino,^[a] Yoshihisa Inoue,^[c] Kazi Aslamuzzaman,^[b] Takeyuki Suzuki,^[d] Said M. Sebti,^[b] and Junko Ohkanda*^[a]

Mutant K-Ras drives cancer through its membrane localization, which requires posttranslational modification by farnesyltransferase (FTase). FTase attaches farnesyl to the K-Ras C-terminal CVIM tetrapeptide, enabling membrane binding. However, K-Ras can also undergo compensatory geranylgeranylation by geranylgeranyltransferase I (GGTase I), making FTase inhibition alone ineffective. Dual inhibition of FTase and GGTase I is necessary to fully block K-Ras localization and its cancer activity. We developed bivalent inhibitors targeting both FTase and GGTase I by binding to the CVIM (C = cysteine, V = valine, I = isoleucine,

M = methionine) site and an adjacent acidic surface. A nonthiol CVIM peptidomimetic based on a piperidine scaffold showed potent FTase inhibition ($K_i = 2.1$ nM) with less effect on GGTase I ($K_i = 210$ nM). Adding cationic modules to this compound produced dual inhibitors with enhanced potency ($K_i = 2\text{--}5$ nM), significantly improving upon previous agents. These bivalent inhibitors effectively reduced mutant K-Ras cancer cell viability and inhibited K-Ras farnesylation and geranylgeranylation in cells. This dual-targeting approach shows promise for treating K-Ras-driven cancers.

1. Introduction

Members of the Ras family of 21-kDa GTPases play a pivotal role in the regulation of numerous physiological processes, including proliferation and differentiation. Oncogenic mutations in the Ras proteins result in their constitutive activation and have been identified in approximately 20% of all human cancers. This leads to increased cell-cycle entry, cell growth and survival, and angiogenesis.^[1] K-Ras is the most frequently mutated Ras isoform and is associated with aggressive tumorigenesis in 90% of pancreatic, 50% of colon, and 25% of lung adenocarcinomas,^[2] drug resistance, and poor clinical outcomes.^[3] Despite the considerable challenges posed by the picomolar affinity of Ras

for GTP,^[4] submillimolar intracellular concentrations of GTP,^[5] and the lack of a pocket for small-molecule-binding on the protein surfaces of Ras proteins, pharmaceutical studies targeting the mutated residues of K-Ras with covalent agents have made significant progress in recent years,^[6] including the FDA-approved clinical drugs for the treatment of non-small-cell lung cancer,^[3] highlighting the promise of K-Ras-directed anticancer therapy.^[7] K-Ras-targeted molecular strategies also include macrocyclic peptides,^[8] proteolysis-targeting chimeras,^[9] and reversible inhibitors.^[10] However, there are still challenges regarding resistance and short duration of responses to K-Ras inhibitors.^[3,11] Therefore, alternative approaches for controlling K-Ras activation are needed.

One potential alternative strategy is to inhibit K-Ras prenylation, a lipid post-translational modification that is essential for the proper cellular localization and function of the protein. Protein farnesyltransferase (FTase) and type I geranylgeranyltransferase (GGTase I) are the enzymes responsible for transferring farnesyl and geranylgeranyl groups, respectively, to the thiol group of cysteine of the C-terminal CVIM tetrapeptide motif (C: cysteine, V: valine, I: isoleucine, M: methionine). A number of potent inhibitors for FTase (FTIs) and GGTase I (GGTIs) have been developed over the past several decades.^[12,13] However, their limited efficacy revealed in the clinical trials has highlighted significant challenges in cancer chemotherapeutics by targeting K-Ras prenylation.^[12] Furthermore, FTI treatment has been shown to be ineffective because under the pressure of FTIs, K-Ras becomes geranylgeranylated by GGTase I, resulting in geranylgeranylated K-Ras that retains its full biological functionality.^[14,15]

The aforementioned obstacles have been elucidated by studies that have demonstrated the existence of an electrostatic


[a] N. Horiuchi, F. Sugino, N. Ogino, J. Ohkanda
Academic Assembly, Institute of Agriculture, Shinshu University, 8304
Minami-Minowa, Kami-Ina, Nagano 399-4598, Japan
E-mail: johkanda@shinshu-u.ac.jp

[b] R. Omer, K. Aslamuzzaman, S. M. Sebti
Department of Pharmacology and Toxicology, Massey Comprehensive
Cancer Center, Virginia Commonwealth University, Richmond, VA, USA

[c] Y. Inoue
SDMJ Consulting, Gohongi 2-7-8, Meguro, Tokyo 153-0053, Japan

[d] T. Suzuki
SANKEN, Osaka University, 8-1 Mihogaoka, Ibaraki, Osaka 567-0047, Japan

 Supporting information for this article is available on the WWW under
<https://doi.org/10.1002/chem.202500306>

 © 2025 The Author(s). Chemistry – A European Journal published by
Wiley-VCH GmbH. This is an open access article under the terms of the
Creative Commons Attribution-NonCommercial-NoDerivs License, which
permits use and distribution in any medium, provided the original work is
properly cited, the use is non-commercial and no modifications or
adaptations are made.

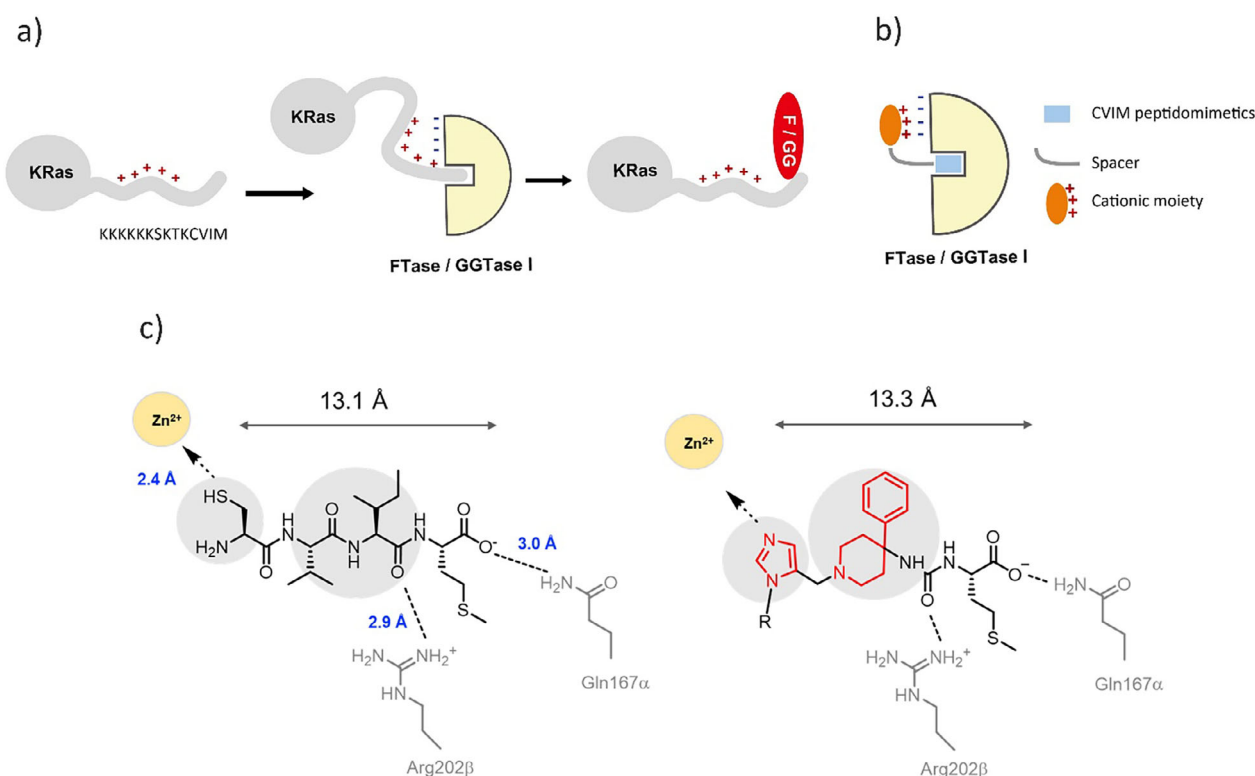


Figure 1. a) Schematic presentation of farnesylation and geranylgeranylation of the cysteine residue of C-terminal CVIM of K-Ras by FTase and GGTase I. b) Dual inhibition strategy for FTase and GGTase I by a bivalent agent that mimics the K-Ras C-terminal oligopeptide containing CVIM and oligo lysine domain. c) Structure-based design of CVIM peptidomimetic containing piperidine scaffold bearing imidazole and methionine residue via an urea linkage.

attraction between the positively charged cationic C-terminal poly-lysine domain of K-Ras (KKKKKKSKTKCVIM) and the common negatively charged anionic surface of FTase and GGTase I^[14–18] as illustrated in Figure 1a. FTase and GGTase I are heterodimeric zinc metalloenzymes, comprising identical 48 kDa α -subunits. The surface area in close proximity to the entrance of each active pocket is characterized by a negatively charged local region of approximately 90 Å², which encompasses a number of acidic residues (Glu125, Glu 160, Glu161, Glu187, Asp191, Glu229, and Asp230).^[18] Indeed, K-Ras exhibits an intrinsic affinity for FTase that is 20 – 50 times higher than that observed for other Ras isoforms.^[16,17]

The mode of the molecular recognition between K-Ras and FTase and GGTase-I, which involves the transient protein-protein interactions driven by the electrostatic interactions, suggests that a bivalent compound mimicking the K-Ras C-terminus KKKKKKSKTKCVIM domain may be developed by linking a CVIM peptidomimetic and a cationic moiety via an appropriately lengthened spacer (Figure 1). This approach may serve to anchor the entire molecule to the active sites of FTase and GGTase I, thereby facilitating the delivery of the cationic moiety to the shared acidic surface. Furthermore, it may act as a dual inhibitor for farnesylation and geranylgeranylation of K-Ras (Figure 1b). Although successful examples of conventional small molecule-based dual inhibitors for FTase and GGTase I have been reported,^[19] a significant challenge in developing these inhibitors lies in the structural difference between the active sites of FTase and GGTase I, particularly around the binding site of “X”

residue in the CAAX (C = cysteine, AA = aliphatic dipeptide, X = methionine, serine, glutamine for FTase, leucine, phenylalanine for GGTase I) peptide. Therefore, we anticipated that targeting the common surface structure with bivalency would be advantageous for the structure-based design of dual inhibitors targeting both enzymes.

We previously demonstrated that a series of bivalent agents, in which a CVIM tetrapeptide was linked to a branched gallate derivative that was highly functionalized by a number of primary amino groups, exhibited significant inhibitory effects on farnesylation and geranylgeranylation. The C-terminal K-Ras peptidomimetic demonstrated greater potency in vitro, exhibiting a 200-fold increase in activity for FTase and a 20-fold increase for GGTase I, respectively, compared to the CVIM tetrapeptide.^[20] Moreover, the introduction of a previously developed thiol-containing peptidomimetic and guanidyl-gallate groups into the bivalent agent resulted in enhanced cell-based activity, leading to the disruption of K-Ras prenylation and its binding to c-Raf at the plasma membrane.^[21] These results support the potential of the bivalent strategy for controlling K-Ras prenylation and consequent growth signaling pathways through the association with downstream effectors, including c-Raf. However, the dual inhibitory potency of the compound remained modest, with a significantly low K_i value for FTase of 0.6 nM, whereas the activity for GGTase I remained in the submicromolar range with a K_i of 0.71 μ M. Moreover, the metabolically susceptible thiol group of the CVIM peptidomimetics and the moderate cell-based activity hampered further biological evaluation, thereby necessitating

the development of non-thiol bivalent agents with enhanced cell-based activity potential.

In this report, we present the structure-based design, synthesis, and functional evaluation of a new series of non-thiol K-Ras proteomimetics based on the piperidine scaffold for the dual inhibition of FTase and GGTase I. These compounds were observed to exhibit potent inhibitory activity against both FTase and GGTase I at low nM concentrations in vitro and to suppress cell growth in a concentration-dependent manner. Moreover, the aniline-containing derivative **4c** was observed to disrupt the processing of both K-Ras and Rap1 in cells, which provides further support for the strategy of binding to the common acidic surface of FTase and GGTase I for dual inhibition in cells.

2. Results and Discussion

2.1. Design and Synthesis of Piperidine-Based CVIM Peptidomimetics

The design of the piperidine-based peptidomimetics for the CVIM tetrapeptide is illustrated in Figure 1c. The crystal structure of the ternary complex of FTase bound to the C-terminal peptide of K-Ras and an analog of farnesyl pyrophosphate reveals that the CVIM occupies a substantial hydrophobic pocket in the enzyme in an extended conformation, forming two hydrogen bonds with Gln167 α and Arg202 β , while the Cys thiol group coordinates with the catalytic zinc ion.^[18] In this study, the free thiol group was replaced with an imidazole group, which has been successfully employed in previous studies as a substitute for zinc coordination.^[22] The hydrophobic Val-Ile dipeptide is replaced by a rigid 4-phenyl piperidine moiety, to which are attached a) the imidazole moiety for coordination to the catalytic zinc ion and b) methionine residue for hydrogen bonding with Gln167 α in the active site of FTase (Figure 1c). In order to maintain a similar distance between the N-3 nitrogen and the methionine carboxylate observed in the crystal structure (~13 Å), a methylene group was selected between the imidazole and the piperidine moiety, and a urea moiety was designed between the piperidine and the methionine as the spacers, respectively (Figure 1c). We anticipated that the carbonyl group of the urea moiety may be located in an optimal position for forming a hydrogen bond with Arg202 β , analogous to the isoleucine amide oxygen of CVIM observed in the crystal structure (Figure 1c).

Accordingly, *N*-nonsubstituted imidazole- (**1**) and *N*-(*p*-azidobenzyl)imidazole-containing piperidine derivatives (**3**) were designed and synthesized (Figure 2). We chose 1,5-benzyl substituted imidazole group as previous study showed a clear structure-activity-relationship that 1,4-substitution of imidazole moiety significantly reduced activity.^[23] In addition, an azido functionality was introduced, via the Huisgen cycloaddition reaction, at *para*-position of the benzyl group for further modification to attach a moiety that binds the negatively charged acidic surface of FTase and GGTase I.

The computational docking model of FTase in complex with **1** and the FPP analog assisted that the N-3 nitrogen of the imidazole group coordinates with the catalytic zinc ion, while the methionine carboxylate and the urea oxygen form a hydrogen bond with Gln167 α and Arg202 β , respectively (Figure 3). In addition, the model predicted noncanonical interactions around the methionine residue in **1** and Tyr131 α , such as S – π and / or CH₃ – π interactions.^[24] Furthermore, the model demonstrates that the phenyl group of the piperidine scaffold occupies a hydrophobic pocket formed by aromatic amino acid residues Trp102 β , Trp106 β , and Tyr361 β , thereby validating our peptidomimetic design.

Synthetic procedures for **1** and **3** are depicted in Scheme 1. Briefly, the Curtius rearrangement of *N*-Boc-protected 4-phenyl-4-piperidine carboxylic acid (**6**) with L-methionine methyl ester resulted in the formation of the corresponding urea derivative (**7**) in a high yield. Following the removal of the Boc group, reductive amination of the resulting free piperidine derivative and imidazole-4-carboxyaldehyde or *N*-(*p*-azidobenzyl)imidazole-5-carboxyaldehyde using sodium triacetoxyborohydride gave the methyl ester prodrugs **8** and **2**, which were subsequently hydrolyzed to afford the free acid forms **1** and **3**, respectively.

2.2. In vitro Inhibition Activity of Piperidine-Based CVIM Peptidomimetics for FTase and GGTase I

The inhibition activities of **1** and **3** of recombinant FTase and GGTase I were evaluated using a previously reported fluorescent spectroscopic assay^[25] with an environmentally sensitive fluorogenic substrate, the dansyl-labeled K-Ras C-terminal peptide (K)₆SK(Dans)TKCVIM (Dans = ω -*N*-dansyl) as a substrate. As a result, the *N*-nonsubstituted derivative **1** was shown to exhibit moderate inhibition activity against FTase in a concentration-dependent manner (*K*_i = 790 nM, Figure 4, Table 1), whereas it had no activity against GGTase I (> 500,000 nM), indicating that **1** is a selective inhibitor for FTase over GGTase I. By contrast, the *N*-(*para*-azidobenzyl) derivative **3** demonstrated a remarkably enhanced potency for FTase (*K*_i = 2.1 nM), exhibiting a 376-fold increase in potency compared to **1**. In addition, **3** was observed to inhibit geranylgeranylation of the K-Ras model peptide but with a much lower potency (*K*_i = 210 nM). These results strongly indicate that the *para*-azidobenzyl group of **3** enhances hydrophobic interaction in the active pocket of FTase and GGTase I, resulting in improved dual inhibition activity compared to **1**.

2.3. Design and Synthesis of Non-Thiol-Containing Bivalent Agents Based on the Piperidine Scaffold

Given the promising dual potency demonstrated by the (*para*-azidobenzyl)imidazole-attached piperidine derivative **3**, our next objective was to extend this peptidomimetic to the design of bivalent agents that, in addition to binding the CVIM binding pocket of FTase and GGTase I, could potentially mimic the positively charged poly-lysine C-terminus of K-Ras and bind the

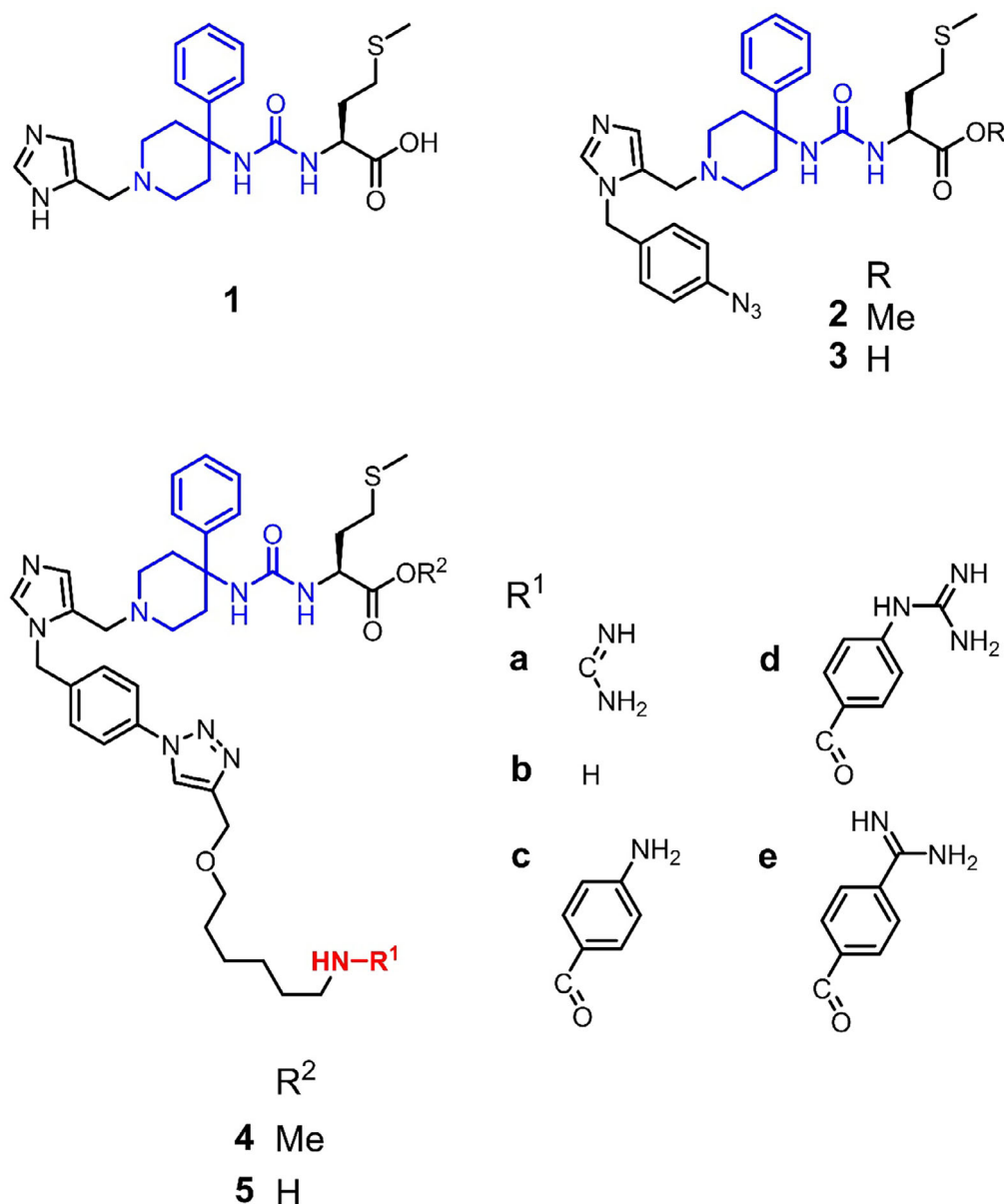


Figure 2. Chemical structures of the series of imidazole-containing piperidine-based proteomimetics 1–5.

negatively charged acidic surface of FTase and GGTase I. We envisioned that the introduction of various cationic moieties via an appropriately lengthened spacer to the *para*-position of the benzyl group in **3**, achieved through the Huisgen cycloaddition, would readily afford **5a–e** for a structure-activity relationship study (Figure 2).

The computational model of FTase bound to **5c** and an FPP analog indicated that the aminohexyloxymethyl group between the triazole C4 position and the substituent R¹ group is an optimal spacer to deliver the cationic moiety in proximity approximately within 3 Å distance to the acidic residues, including Asp59 α , Glu125 α , Glu161 α , and Glu162 α (Figure 5). In line with this model, a series of Boc-protected guanidyl, amino, and amidyl-attached propagyl derivatives **9a–e** were designed for the Huisgen 1,3-dipolar addition with **2**, with the aim of synthesizing the bivalent derivatives **5a–e**.

As depicted in Scheme 2, Boc-protected guanidylation or Boc protection of 6-amino-1-hexanol, followed by Williamson ether synthesis with propagyl chloride, afforded **9a** and **9b**, respectively. The removal of Boc group of **9b** was followed by amide condensation with Boc-protected 4-amino, 4-guanidyl, or 4-amidyl benzoic acid, which gave **9c–e**, respectively. In order to prepare a control compound, **9a** and **9e** were deprotected to give the free guanidyl **12** and amidyl derivatives **13**, respectively. The resulting Boc-protected derivatives **9a–e** were subjected to the Huisgen cycloaddition reaction with **2** under standard conditions, and fully protected conjugates **14a–e** were obtained in excellent yields. Subsequently, the Boc groups were removed through acid treatment, resulting in the formation of the corresponding methyl ester forms **4a–e**. These were then subjected to hydrolysis, yielding the free acid forms **5a–e**, respectively (Scheme 3).

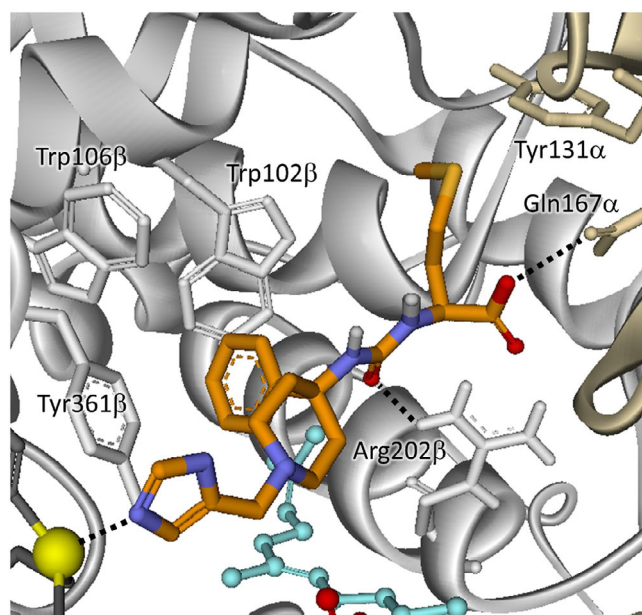


Figure 3. A docking model of **1** (orange stick) bound to FTase (IMZC: α , β subunits, gold and gray ribbons), FPP analogue (ball and stick), Zinc (yellow sphere), Tyr131 α , and Gln167 α (gold stick), Trp102 β , Trp106 β , and Arg202 β (gray stick) are highlighted (Glide in Schrodinger Suites 2015-2).

2.4. In vitro Inhibition Activity of Piperidine-Based Bivalent Proteomimetics for FTase and GGTase I

The inhibitory activities of bivalent compounds **5a–e** were evaluated using the fluorescent spectroscopic assay described in the previous section. The guanidyl derivative **5a** exhibited high

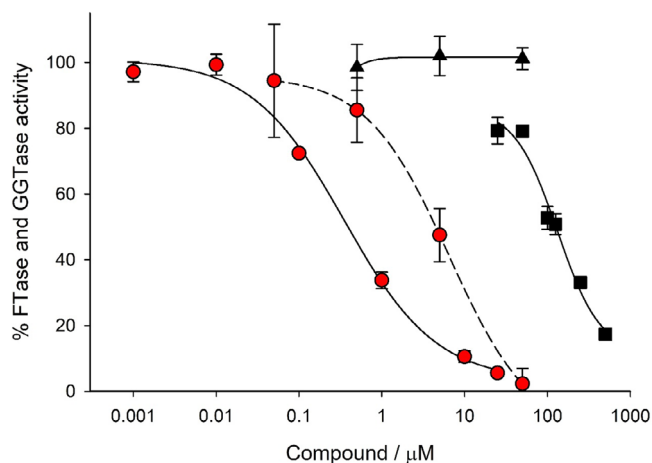
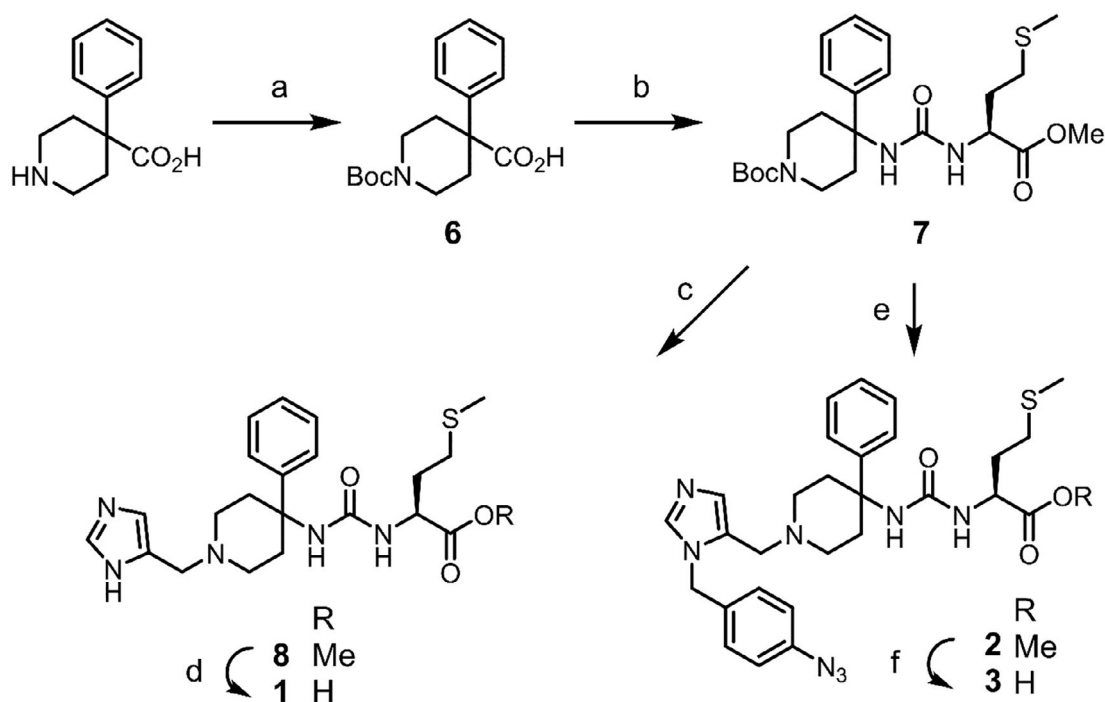


Figure 4. Dose-response curves for the inhibition of FTase (solid line) by **1** (black squares), **3** (red circles), and **12** (black triangles), and GGTase I (dashed line) by **3** (blue circles). Fluorescent in vitro assays were carried out by using KKKKKKSK(Dans)TKCVIM (1 μ M) and FPP (5 μ M) in 50 mM Tris-HCl, pH 7.5, at 37 $^{\circ}$ C. $n = 3$. Mean values \pm SEM are shown.

potency for FTase and was also highly selective for FTase over GGTase I (147-fold) with a K_i value of 1.7 and 250 nM, respectively (Figure 6a, Table 1). This was comparable to **3** that was 100-fold selective for FTase (K_i of 2.1 nM) over GGTase I (K_i of 210 nM). Similarly, monoamine derivative **5b** was found to be equally active as **5a** for FTase (K_i of 3.8 nM), and 20-fold selective for GGTase I (K_i of 77 nM). These results indicate that the introduction of the guanidyl or the monoamino group at the surface module did not result in significant improvements in dual inhibition activity, suggesting that the electrostatic interaction between these



Scheme 1. Synthesis of **3** and **4**. (a) Boc_2O , dioxane, NaOH, 85%; (b) DPPA, H-Met-OMe, quant.; (c) TFA, then imidazole-4-carboxyaldehyde, sodium triacetoxyborohydride, 32%; (d) KOH, methanol, 33%; (e) TFA, then *N*-(*p*-azidobenzyl)imidazole-5-carboxyaldehyde, sodium triacetoxyborohydride, 60%; (f) KOH, methanol, 96%.

Table 1. Inhibition of prenylation of the K-Ras C-terminal peptide by FTase and GGTase I.^[a]

Cmpd	K_i (IC_{50}), nM ^[b]	
	FTase	GGTase I
1	790 ± 45 (13,200 ± 7400)	- (> 500,000)
3	2.1 ± 0.50 (350 ± 90)	210 ± 0.00 (6480 ± 0.00)
5a	1.7 ± 0.50 (290 ± 80)	250 ± 50 (7840 ± 1580)
5b	3.8 ± 1.1 (630 ± 190)	77 ± 51 (2400 ± 1600)
5c	4.6 ± 0.08 (752 ± 1.34)	2.9 ± 0.70 (90 ± 2.0)
5d	1.8 ± 0.40 (300 ± 70)	3.1 ± 0.50 (96 ± 14)
5e	2.0 ± 0.20 (330 ± 40)	17 ± 5.0 (530 ± 160)
12	- (> 500,000)	- (>50,0000)
13	- (>500,000)	- (>500,000)

^[a] Fluorescent in vitro assays were performed in a 96-well black plate using KKKKKKSK(Dans)TKCVIM (1 μ M), farnesyl pyrophosphate (FPP, 5 μ M), compounds (0–500 μ M), and enzyme (25–37 nM) in 50 mM Tris HCl (pH 7.5) at 37 °C. The reaction was monitored at 520 nm (ex. 340 nm) for 5 minutes with a plate reader. SEM is given for $n = 3$.

^[b] K_i values were obtained by conversion of IC_{50} values shown in parentheses using the Cheng-Prusoff equation (ref.[39]), $K_i = IC_{50}/[1 + ([S]/K_M)]$, where for FTase $K_M = 0.006 \pm 0.002 \mu$ M and for GGTase I $K_M = 0.0033 \pm 0.008 \mu$ M (ref.[20]).

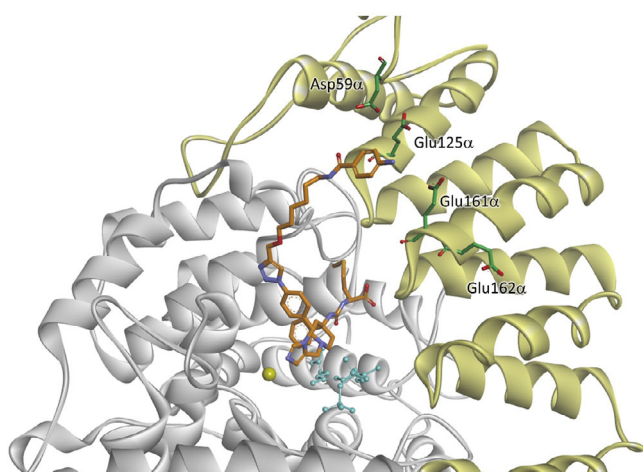


Figure 5. A docking model of **5c** (orange stick) bound to FTase (1M2C: α , β subunits, gold and gray ribbons). zinc (yellow sphere), FPP analogue (ball and stick), Asp59 α , Glu125 α , 161 α , and Glu162 α (green stick) are highlighted. First, a model compound in which the azido group in **3** was replaced by triazole group was docked into the active pocket FTase by Glide in Schrodinger Suites 2015-2, and the aniline-containing spacer moiety was added to 4-position of the triazole group.

functional groups and the acidic residues on the surface of FTase and GGTase I was insufficient to enhance the binding affinity to the enzymes. In contrast, a notable enhancement in the inhibitory activity against GGTase I was observed for **5c–e**, which possesses a substituted phenyl ring moiety in its surface binding module (Figure 6b). In particular, the aniline-containing derivative **5c** and the phenylguanidino group-containing derivative **5d** exhibited remarkable dual inhibitory activities with single-digit nM K_i values (**5c**: 4.6 nM for FTase, 2.9 nM for GGTase I; **5d**: 1.8

nM for FTase, 3.1 nM for GGTase I, Table 1), with these compounds being approximately one order of magnitude more potent for GGTase I than **5a**. It is noteworthy that their activities against GGTase I are approximately 230 times more potent than that of the previously developed guanidyl-gallate derivative.^[21]

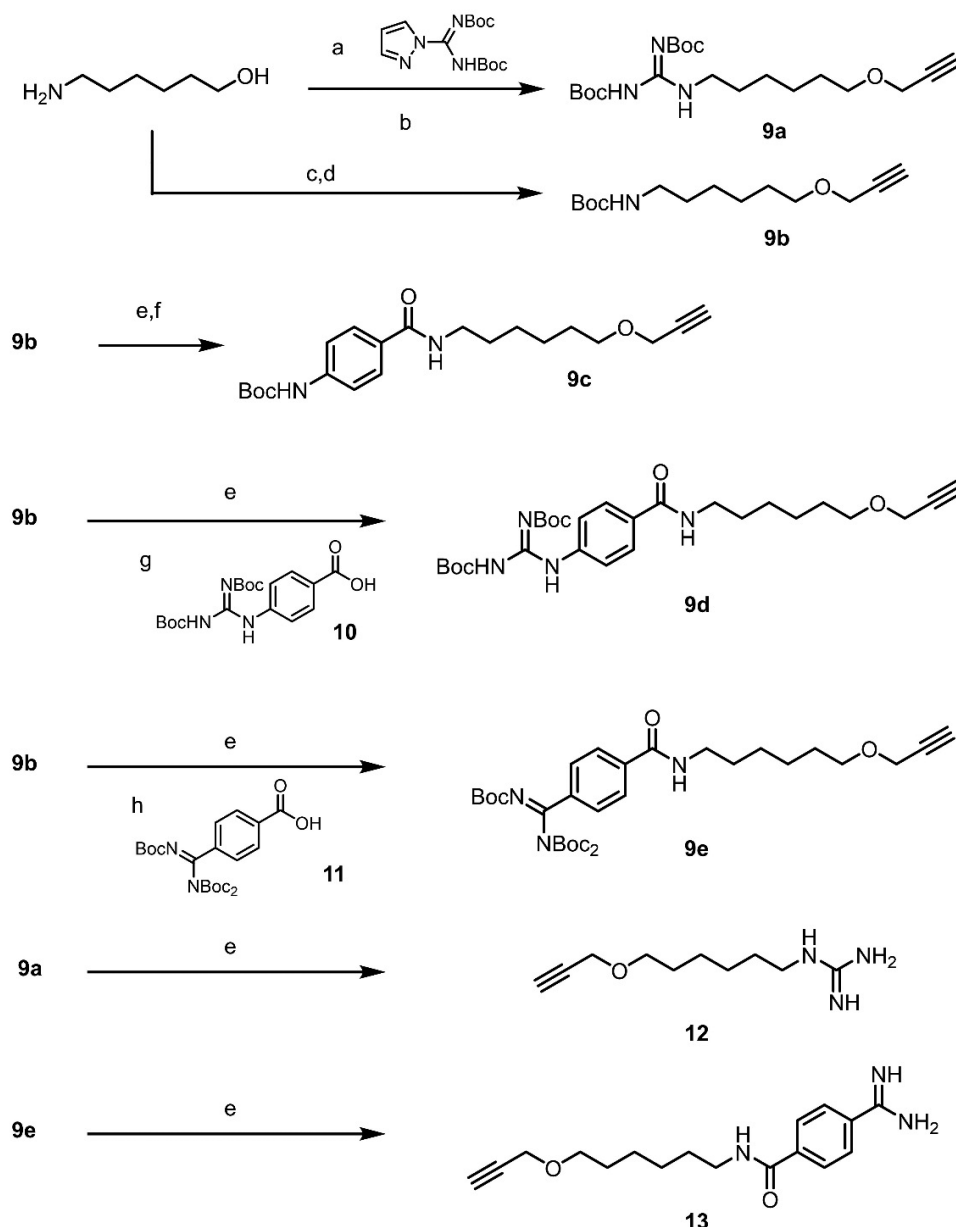
To evaluate the impact of the aromatic ring system on potency, a superimposed model of **5c** and GGTase I was analyzed (Figure 7). The model shows that GGTase I has several distinctive aromatic residues (e.g., Tyr40, His316, and Trp312) on the surface of the β -subunit, situated near the entrance of the active site. These are accompanied by proximal acidic residues, including Glu38 β , and Asp314 β . The model also indicates that these residues are likely to be available for aromatic and electrostatic interactions with the anilino group in **5c**. As these residues are exclusive to GGTase I, not FTase, it is likely that interactions involving such residues are responsible for the positive effect on improving inhibition activity for GGTase I, while maintaining potency for FTase.

2.5. Antiproliferative Activity Against Pancreatic Cancer Cells

Next, we assessed whether these compounds inhibit cell proliferation, as has been reported for FTIs.^[26,27] To this end, the corresponding methyl esters **2** and **4a–e** were used, as previous studies have demonstrated that ester prodrugs significantly improve cell-based activity.^[28] Briefly, human pancreatic carcinoma MiaPaCa2 cells that harbor a K-Ras G12C mutation were treated with the compound and incubated for three days prior to a trypan blue assay. We used sotorasib (AMG510, Figure S1),^[29] a covalent K-Ras G12C inhibitor, as a positive control, and the results are shown in Figure 8. The peptidomimetic **2** demonstrated concentration-dependent antiproliferation activity, with an IC_{50} value of approximately 0.1–1 μ M, which was approximately 10-fold higher than that of sotorasib ($IC_{50} = 0.01 \sim 0.1 \mu$ M). All bivalent compounds demonstrated the ability to suppress cell growth, while the propargyl derivative **13** was found to be inactive, suggesting that the observed antiproliferative activity is caused by the ability of compounds to potently inhibit FTase in vitro (Table 1) and farnesylation in cells.

2.6. Effect on Processing of K-Ras, HDJ-2, and Rap1 in Cells

Finally, the compounds were evaluated for their inhibitory activity against protein prenylation in cells through a gel-shift assay, which enabled the separation of prenylated and unprenylated proteins (Prenylated proteins migrate faster than unprenylated proteins in SDS-PAGE gels as documented previously.^[12,19,30] Previously developed dual inhibitor FGTI-2734 (FGTI, Figure S1)^[19] was utilized as a positive control. Briefly, MiaPaca-2 cells were treated with the indicated compounds for 48 hours and the cell lysates were processed for SDS-PAGE western blot using anti-K-Ras, -HDJ-2, or Rap1 antibodies (Figure 9). Note that HDJ-2, a 40 kDa heat shock protein with the C-terminal CQTS sequence, is a substrate for FTase, and is exclusively farnesylated. Rap1, a Ras-related GTPase with the C-terminal CLLL sequence, is a



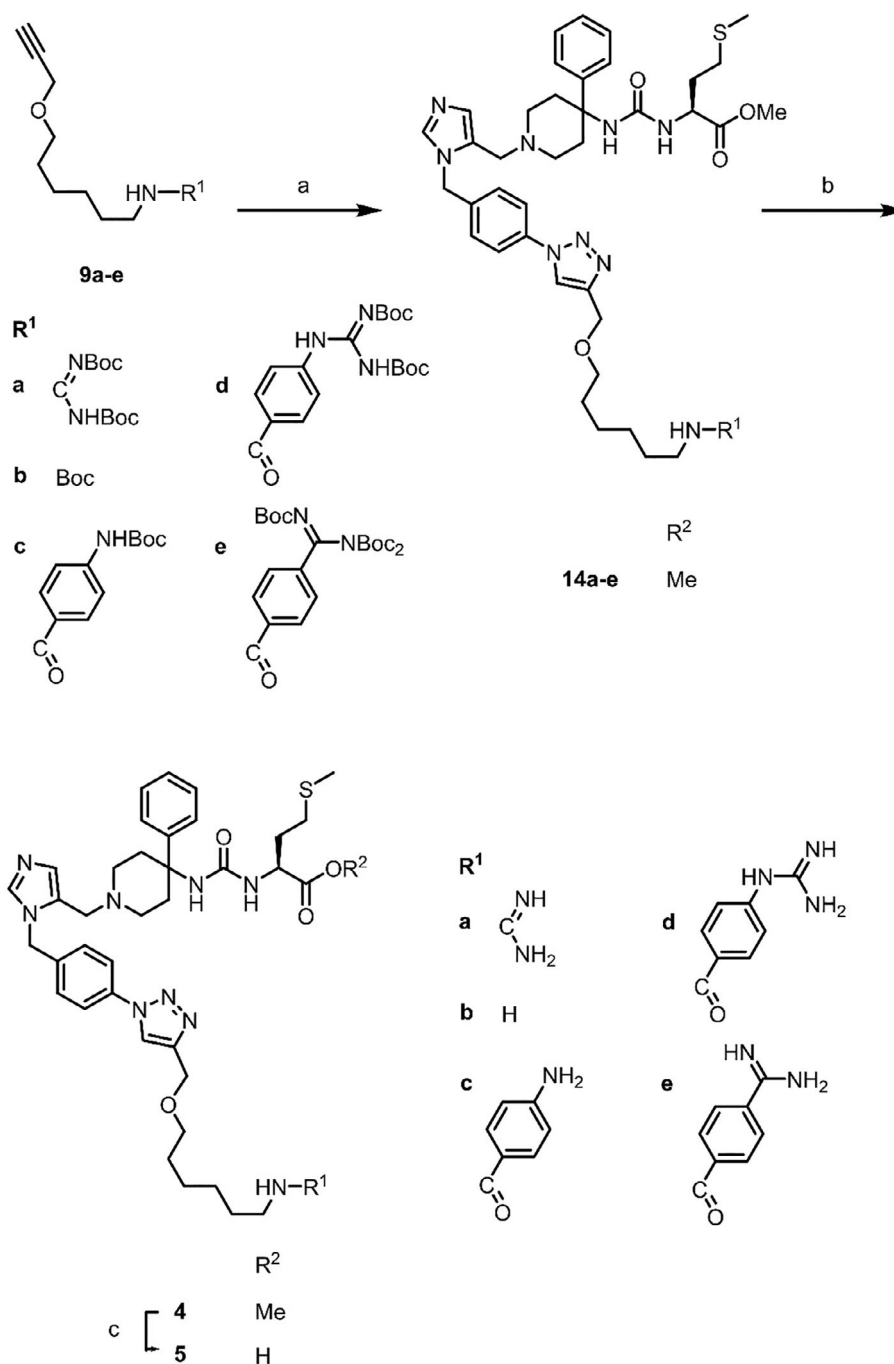
Scheme 2. Synthesis of Boc-protected propagyl derivatives **9a-e**, and free **12** and **13**. (a) (Boc)₂-1H-pyrazole-1-carboximidamide, TEA, DCM, quant. (b) propagyl bromide, NaH, THF, 73%. (c) Boc₂O, NaOH, dioxane, 84%. (d) propagyl bromide, NaOH, THF, 73%. (e) TFA, dichloromethane. (f) *N*-Boc-4-aminobenzoic acid, PyBop, HOBt, TEA, DCM, 73%. (g) **10**, PyBop, HOBt, TEA, DCM, 77%. (h) **11**, PyBop, HOBt, TEA, DCM, 57%.

substrate for GGTase I and is exclusively geranylgeranylation. In contrast, K-Ras is normally farnesylated but when FTase is inhibited, it becomes geranylgeranylated by GGTase I. Figure 9 shows that all compounds inhibited the farnesylation of HDJ-2, which is consistent with the compounds nanomolar inhibition potency against FTase in vitro (Table 1). In contrast, only **2** and **4c** inhibited the geranylgeranylation of Rap1 with **4c** being more potent than **2**, consistent with its much higher potency against GGTase I in vitro (Table 1). Although compounds **4d** and **4e** are potent GGTase I inhibitors in vitro, they did not inhibit Rap1 geranylgeranylation in cells, possibly due to being metabolically modified in cells leading to their inability to inhibit GGTase I while keeping their ability to inhibit FTase. Consistent with this, only compounds **2** and **4c** that were able to inhibit both far-

nesylation and geranylgeranylation in cells were also able to inhibit the prenylation of K-Ras (Figure 9, the top panel) that requires simultaneous inhibition of both FTase and GGTase-1 to fully abrogate K-Ras prenylation and membrane localization. Overall, these results demonstrate that the bivalent compound **4c** has the potential to serve as a lead compound for the dual inhibition of K-Ras farnesylation and geranylgeranylation in cells.

3. Conclusions

In this study, we developed a new non-thiol, piperidine-based CVIM-peptidomimetic **3**, which possesses a *p*-azido benzyl



Scheme 3. Synthesis of bivalent compound **4** and **5**. (a) **2**, **9**, ascorbic acid, CuSO₄, tris-hydroxypropyltriazolylmethylamine, THF: H₂O = 3:2, 79% ~ quant. (b) TFA, DCM, quant. (c) 0.1N KOH, methanol, 22% ~ quant.

imidazole moiety, and exhibited low nanomolar potency for FTase in vitro. Further elaboration of **2** was achieved through the linkage of a cationic surface-binding module via Huisgen cycloaddition to afford the bivalent series of compounds. In particular, compounds containing an aromatic ring system (**5c-d**) were demonstrated to possess high potency as dual inhibitors for FTase and GGase I, exhibiting a single-digit nM *K_i* value. Only the surface module itself did not cause much of an effect on inhibiting K-Ras prenylation. These results support the assertion that the bivalent strategy, which enables simultaneous binding to the CVIM active pocket and the acidic surfaces of

the enzymes, enhances dual inhibitory FTase and GGase I activities. Furthermore, the methyl ester prodrugs **2** and **4c**, were demonstrated to inhibit the processing of K-Ras and Rap 1, suggesting that these compounds may serve as potential lead compounds for the further development of the dual inhibitors that target the lipid modification of K-Ras.

Although the presented compounds show promise, their overall cellular activity remains moderate, likely due to limited cell permeability. Further structure-activity-relationship studies, including modifications to the spacer length, will be essential to enhance their activity.

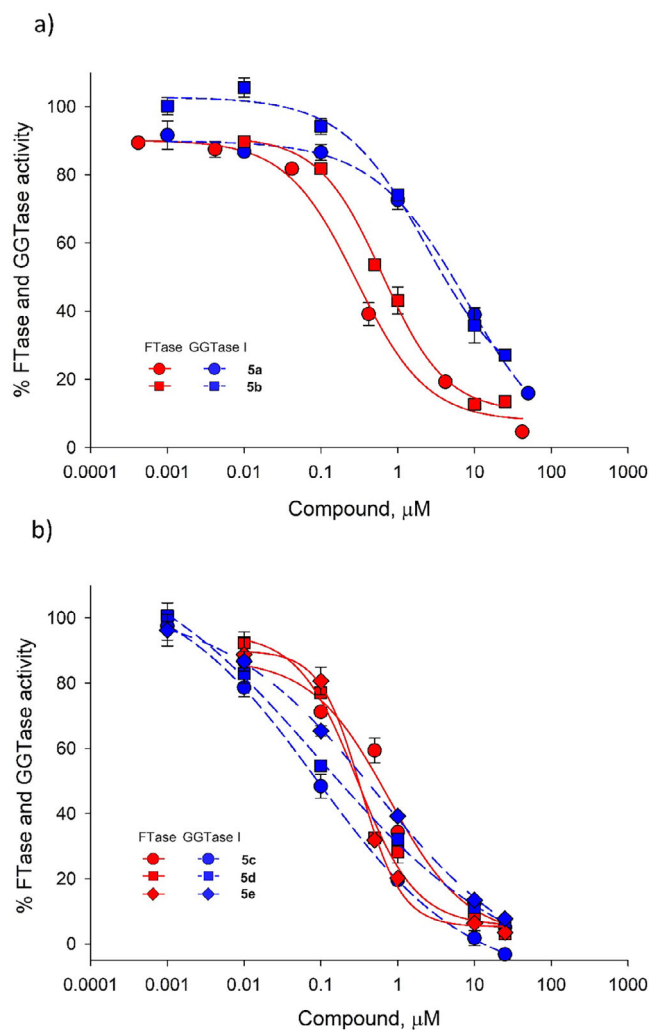


Figure 6. Dose-response curves for the inhibition of FTase (red solid) and GGTase I (blue dash) by a) **5a** (circles) and **5b** (squares), and by b) **5c** (circles), **5d** (squares), and **5e** (diamonds). Fluorescent in vitro assays were carried out by using KKKKKKSK(Dans)TKCVIM (1 μ M) and FPP (5 μ M) in 50 mM Tris-HCl, pH 7.5, at 37 $^{\circ}$ C. $n = 3$. Mean values \pm SEM are shown.

The bivalent dual inhibitors with low nanomolar activity presented in this study may provide insights into a new approach for developing K-Ras-targeting antitumor therapeutics.

4. Experimental Section

Chemistry: Reagents and solvents were obtained from commercial sources (TCI, FUJIFILM Wako Pure Chemical Corporation, Nacalai Tesque, Sigma-Aldrich, or Kanto Chemical) and used without further purification unless otherwise noted. Flash column chromatography was performed on silica gel (38–100 μ m) under a pressure of about 4 psi. ^1H and ^{13}C NMR spectra were recorded on AVANCE NEO 400 spectrometer. Chemical shifts were reported in δ (ppm) relative to tetramethylsilane. Coupling constants were reported in hertz (Hz). Analytical HPLC was performed by JASCO PU-4185 binary pump equipped with JASCO UV-4075 UV/Vis detector and a COSMOSIL (38144-31) Packed column (5C18-AR – II, 4.16ID \times 150 mm) with gradient eluent (H_2O and methanol, 10–90% in 20 minutes) at a flow rate of 1 mL/min. Preparative LC was performed by SHI-

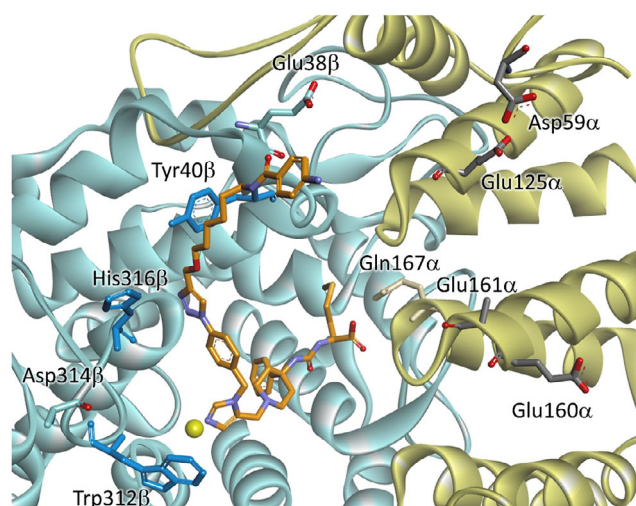


Figure 7. A computational model of **5c** (orange stick) bound to GGTase I (α and β subunits, gold and light blue ribbons) is presented. The model highlights the following: zinc (yellow sphere), typical acidic residues on the α -subunit surface (stick), aromatic residues on the β -subunit near the entrance (blue stick), and Glu38 β and Asp314 β (light blue stick). The model was generated through superimposition of the model of the ternary complex of FTase bound to **5c** (Figure 5) with the crystal structure of GGTase I bound to the K-Ras SKCVIM peptide (1TNO), overlaying the positions of each catalytic zinc ion, and the methionine residues in **5c** and in the SKCVIM ligand. FTase, FPP and GGPP analogues, as well as the SKCVIM ligand have been omitted for clarity.

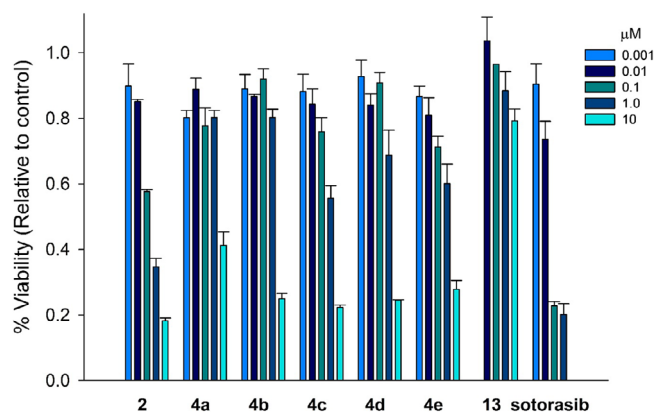


Figure 8. Antiproliferative activity for MiaPaCa2 cells. Cells (1×10^3 cells) were treated with **2**, **4a–e**, **13**, or sotorasib and incubated at 37 $^{\circ}$ C, 5% CO_2 for 72 hours prior to a trypan blue assay. $n = 3$. Mean values \pm SEM are shown.

MADZU LC-10AT VP equipped with SHIMADZU SPD-10A VP UV/Vis detector and an Inertsil ODS column (GL Sciences Inc. (5020-06823) 5 μ m 20 \times 100 mm). High-resolution mass spectra (HRMS) were recorded by LTQ Orbitrap XL (THERMO) at SANKEN Comprehensive Analysis Center of Osaka University. *N*-(*p*-azidobenzyl)imidazole-5-carboxyaldehyde [3054789-43-1] was synthesized according to the procedure reported in literature.

1-(tert-Butoxycarbonyl)-4-phenylpiperidine-4-carboxylic acid (6): To a solution of 4-phenyl-4-carboxy-piperidine tosylate (5 g, 13 mmol) and 2N NaOH (20 mL, 40 mmol, 3 equiv.) in dioxane (20 mL) was added Boc₂O (2.6 g, 12 mmol 0.9 equiv.) in THF (12 mL) and the resulting mixture was stirred at r.t. overnight. The mixture was diluted with ethyl acetate (80 mL) and the organic layer was

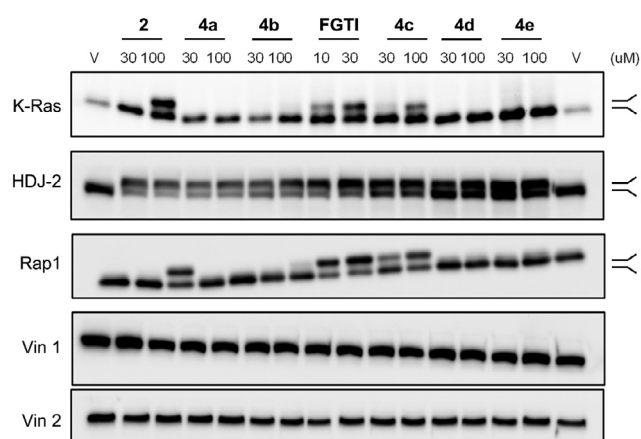


Figure 9. The inhibition activities of **2** and bivalent **4a–e** against prenylation of K-Ras, HDJ-2, and Rap1 (Change in Figure as well) were evaluated using gel shift assays. The dual FTase and GGase I inhibitor FGTI (FGTI-2734)^[19] was used as a positive control. Miapaca-2 cells were treated for 48 hours with vehicle (V) or the indicated compounds at 30 and 100 μM (10 and 30 μM for FGTI-2734), harvested and processed for SDS-PAGE Western blotting with K-Ras, HDJ-2, and Rap1 antibodies as described in the Methods section. The inhibition of prenylation of K-Ras, HDJ-2, and Rap1 was seen by the shift in bands from prenylated (P) to prenylated (U) proteins. Vinculin 1 and 2 were used loading controls.

washed with sat. KHSO_4 (20 mL), H_2O , and brined, and dried over anhyd. Na_2SO_4 . After filtration, the organic solvent was evaporated to give a crude solid, which was then recrystallized from EtOH and H_2O to afford the desired product as a colorless solid (3.45 g, 85%). $^1\text{H-NMR}$ (500 MHz, CDCl_3): δ ppm 7.40 (d, 2H, $J = 7.5$ Hz, aryl), 7.35 (t, 2H, $J = 7.5$ Hz, aryl), 7.28 (d, 1H, $J = 7.5$ Hz, aryl), 3.91 (br s, 2H, piperidine), 3.10 (br s, 2H, piperidine), 2.50 (d, 2H, $J = 13.5$ Hz, piperidine), 1.87 (t, 2H, $J = 2.0$ Hz, piperidine), 1.44 (s, 9H, Boc). $^{13}\text{C-NMR}$ (100 MHz, CDCl_3): δ ppm 178.97, 154.87, 141.44, 128.75, 127.51, 125.97, 79.70, 49.11, 33.35, 28.43. HRMS (ESI): $[\text{M}+\text{Na}]^+$ $\text{C}_{17}\text{H}_{23}\text{NO}_4\text{Na}$ calcd for 328.1525, found 328.1513.

tert-Butyl (S)-4-(3-(1-methoxy-4-(methylthio)-1-oxobutan-2-yl)ureido)-4-phenylpiperidine-1-carboxylate (7): To a solution of **6** (100 mg, 0.33 mmol) and triethylamine (51 μL , 0.36 mmol) in toluene (2 mL) was added diphenyl phosphorazidate (DPPA) (79 μL , 0.36 mmol) and the resulting mixture was stirred at 120 $^\circ\text{C}$ for 2 hours. The reaction mixture was cooled and added L-methionine methyl ester (80 mg, 0.40 mmol) and *N,N*-diisopropylethylamine (DIEA) (67 μL , 0.39 mmol), and the mixture was further stirred at r.t. overnight. The reaction was quenched by adding ethyl acetate and sat. NH_4Cl , and the organic layer was washed with brine, and dried (anhyd. Na_2SO_4). Evaporation and silica gel column chromatography (hexanes: ethyl acetate = 1:1) afforded desired product as a pale yellow amorphous solid (154 mg, quant.). $^1\text{H-NMR}$ (500 MHz, CDCl_3): δ ppm 7.40 (d, 2H, $J = 7.5$ Hz, aryl), 7.33 (t, 2H, $J = 7.5$ Hz, aryl), 7.23 (t, 1H, $J = 7.5$ Hz, aryl), 5.51 (br, 1H, urea), 4.43 (m, 1H, Met- α), 4.00 (br, 2H, piperidine), 3.70 (s, 3H, Met- COOCH_3), 3.11 (br, 2H, piperidine), 1.99 (m, 1H, piperidine, Met- $\text{CH}_2\text{-CH}_2\text{-S-CH}_3$), 1.46 (s, 9H, Boc). $^{13}\text{C-NMR}$ (100 MHz, CDCl_3): δ ppm 173.47, 157.20, 154.81, 146.38, 129.80, 128.53, 126.94, 125.28, 125.08, 79.65, 55.62, 53.54, 52.25, 52.01, 40.15, 39.13, 32.08, 29.76, 28.48, 15.35. HRMS (ESI): $[\text{M}+\text{H}]^+$ $\text{C}_{23}\text{H}_{36}\text{N}_3\text{O}_5\text{S}$ calcd for 466.2375, found 466.2371.

((1-((1H-Imidazol-5-yl)methyl)-4-phenylpiperidin-4-yl)carbamoyl)-L-methionine (1): Compound **7** (100 mg, 0.22 mmol) was treated in 30% trifluoroacetic acid (TFA) in dichloromethane (1.3 mL) at 0

$^\circ\text{C}$ for 30 minutes and concentrated. The deprotected compound was extracted with chloroform and sat. NaHCO_3 , and the organic layer was dried (anhyd. Na_2SO_4) and concentrated. The resulting free piperidine derivative (89 mg) and imidazole-4-carboxyaldehyde (21 mg, 0.22 mmol) were dissolved in dichloromethane (1.5 mL), and the mixture was stirred at r.t. for 30 minutes. The mixture was then added to sodium triacetoxyborohydride (135 mg, 0.644 mmol) at 0 $^\circ\text{C}$, and stirred at r.t. overnight. The product was extracted with chloroform and sat. NaHCO_3 , and the organic layer was dried (anhyd. Na_2SO_4) and concentrated. The crude material was purified by silica gel column chromatography (methanol: chloroform = 1:5 to 0.2 M NH_3 in methanol: chloroform = 1:5) to afford the desired product (**8**) as a colorless amorphous solid (35 mg, 32%). $^1\text{H-NMR}$ (500 MHz, CDCl_3): δ ppm 7.66 (s, 1H, imidazole), 7.39 (d, 2H, aryl), 7.29 (t, 2H, aryl), 7.17 (t, 1H, aryl), 7.06 (s, 1H, imidazole), 4.31 (q, 1H, Met- α), 3.70 (s, 3H, Met- COOCH_3), 3.67 (s, 2H, N- CH_2 -imidazole), 2.89 (m, 2H, piperidine), 2.53 (m, 4H, piperidine), 2.30 (m, 2H, piperidine), 2.06 (m, 6H, C- $\text{CH}_2\text{-CH}_2\text{-SCH}_3$), 1.87 (m, 1H, C- $\text{CH}_2\text{-CH}_2\text{-S-CH}_3$) HRMS (ESI): $[\text{M}+\text{Na}]^+$ $\text{C}_{22}\text{H}_{31}\text{N}_5\text{O}_3\text{SNa}$ calcd for 468.2046, found 468.2033.

A solution of **8** (35 mg, 0.079 mmol) and 2N KOH (393 μL , 0.79 mmol) in methanol (3 mL) was stirred at r.t. until the starting material disappeared on HPLC. After 6 hours, the reaction was quenched by adding 2N HCl (500 μL), and the mixture was concentrated. The product was isolated by solid-phase extraction using a C18 column (10% methanol in dichloromethane to dichloromethane). The crude product (37 mg) was further purified by preparative HPLC to give the desired product as a colorless solid (13 mg, 33%). $^1\text{H-NMR}$ (400 MHz, $\text{DMSO}-d_6$): δ ppm 8.62 (s, 1H, imidazole), 7.64 (s, 1H, imidazole), 7.34–7.30 (m, 4H, aryl), 7.23 (t, 1H, $J = 5.7$ Hz, aryl), 6.83 (s, 1H, imidazole), 6.36 (d, 1H, $J = 7.3$ Hz, urea), 4.43 (s, 2H, N- CH_2 -imidazole), 4.11 (d, 1H, $J = 4.0$ Hz, Met- α), 3.39 (d, 2H, $J = 4.0$ Hz, piperidine), 3.18 (t, 2H, $J = 8.8$ Hz, piperidine), 2.44 (t, 2H, $J = 7.1$ Hz, $-\text{CH}_2\text{-CH}_2\text{-SCH}_3$), 2.17 (d, 2H, $J = 9.8$ Hz, piperidine), 2.02 (s, 3H, $-\text{CH}_2\text{-SCH}_3$), 1.8 (m, 1H, C- $\text{CH}_2\text{-CH}_2\text{-S}$), 1.82–1.74 (m, 1H, C- $\text{CH}_2\text{-CH}_2\text{-S}$). $^{13}\text{C-NMR}$ (100 MHz, $\text{DMSO}-d_6$): δ ppm 174.1, 158.7, 158.4, 157.1, 146.1, 136.2, 128.2, 126.7, 125.3, 124.9, 120.8, 53.7, 51.4, 50.1, 47.9, 39.5, 33.0, 31.8, 29.5, 14.7. HRMS (ESI): $[\text{M}+\text{H}]^+$ $\text{C}_{21}\text{H}_{30}\text{N}_5\text{O}_3\text{S}$ calcd for 432.2069, found 432.2057.

Methyl ((1-((1-(4-azidobenzyl)-1H-imidazol-5-yl)methyl)-4-phenylpiperidin-4-yl)carbamoyl)-L-methionine (2): Compound **7** (415 mg, 0.89 mmol) was deprotected by the procedure described for **8**. The resulting free amine and *N*-(*p*-azidobenzyl)imidazole-5-carboxyaldehyde (184 mg, 0.81 mmol) were dissolved in a mixture of dichloroethane (3 mL) and toluene (3 mL) and heated at 120 $^\circ\text{C}$ for 30 minutes. The solution was concentrated to remove toluene, and the residual imine was dissolved in dichloroethane (4 mL). To the solution was added sodium triacetoxyborohydride (1.06 g, 4.0 mmol) at 0 $^\circ\text{C}$, and the mixture was stirred at 0 $^\circ\text{C}$ to r.t. overnight. Additional sodium triacetoxyborohydride (1.06 g, 4.0 mmol) was added, and the solution was stirred at r.t. until the imine disappeared on TLC for 4 days. The reaction mixture was quenched by adding sat. NaHCO_3 and powder Na_2CO_3 to adjust pH ~ 9 , and the product was extracted with dichloromethane (100 mL). The combined organic layer was dried (anhyd. Na_2SO_4) and concentrated. The crude material (487 mg) was purified by silica gel column chromatography (dichloromethane: methanol = 40:1 to 0.5% NH_4OH in dichloromethane: methanol = 40:1) to afford the desired product as a pale yellow amorphous solid (272 mg, 60%). $^1\text{H-NMR}$ (500 MHz, CDCl_3): δ ppm 7.57 (s, 1H, imidazole), 7.41 (d, $J = 7.5$ Hz, 2H, aryl), 7.36 (t, 2H, $J = 7.5$ Hz, aryl), 7.28 – 7.25 (m, 1H, aryl), 7.08 (d, 2H, $J = 8.5$ Hz, aryl), 6.98 (s, 1H, imidazole), 6.96 (d, 2H, $J = 8.5$ Hz, aryl), 5.22 (s, 2H, benzyl), 4.45 (m, 1H, Met- α), 3.67 (s, 3H, Met- COOCH_3), 3.34 (s, 2H, N- CH_2 -imidazole), 2.59 (m, 2H,

piperidine), 2.25 (m, 4H, piperidine), 1.98 (m, 5H, CH₂-S-CH₃), 1.78 (m, 2H, Met(α)-CH₂). ¹³C-NMR (500 MHz, CDCl₃): δ ppm 173.36 156.44 139.79 138.82 133.48 129.80 128.74 128.37 128.09 127.25 125.27 119.40 5.89 55.21 52.32 52.10 51.87 49.06 48.91 48.37 37.17 35.46 32.09 29.69 25.06 15.56 15.44. HRMS (ESI): [M+H]⁺ C₂₉H₃₇N₈O₃S calcd for 577.2709, found 577.2701.

((1-((1-(4-Azidobenzyl)-1H-imidazol-5-yl)methyl)-4-phenylpiperidin-4-yl)carbamoyl)-L-methionine (3): Compound **2** (30 mg, 0.05 mmol) was hydrolyzed by a similar procedure described for **1** to afford the desired product as a pale yellow amorphous solid (28 mg, 96%). ¹H-NMR (500 MHz, CDCl₃): δ ppm 7.57 (s, 1H, imidazole), 7.41 (d, J = 7.5 Hz, 2H, aryl), 7.36 (t, 2H, J = 7.5 Hz, aryl), 7.28 – 7.25 (m, 1H, aryl), 7.08 (d, 2H, J = 8.5 Hz, aryl), 6.98 (s, 1H, imidazole), 6.96 (d, 2H, J = 8.5 Hz, aryl), 5.22 (s, 2H, benzyl), 4.45 (m, 1H, Met- α), 3.67 (s, 3H, Met-COOCH₃), 3.34 (s, 2H, N-CH₂-imidazole), 2.59 (m, 2H, piperidine), 2.25 (m, 4H, piperidine), 1.98 (m, 5H, CH₂-S-CH₃), 1.78 (m, 2H, Met(α)-CH₂). ¹³C-NMR (500 MHz, CDCl₃): δ ppm 173.36 156.44 139.79 138.82 133.48 129.80 128.74 128.37 128.09 127.25 125.27 119.40 5.89 55.21 52.32 52.10 51.87 49.06 48.91 48.37 37.17 35.46 32.09 29.69 25.06 15.56 15.44. HRMS (ESI): [M+H]⁺ C₂₉H₃₇N₈O₃S calcd for 577.2709, found 577.2701.

N, N-di-Butoxycarbonyl-1-(6-(prop-2-yn-1-yloxy)hexyl)guanidine (9a): To a solution of 6-amino-1-hexanol (100 mg, 0.85 mmol) and triethylamine (0.12 mL, 0.85 mmol) in dichloromethane (5 mL) was added (Boc)₂-1H-pyrazole-1-carboximidamide (400 mg, 1.28 mmol) and the mixture was stirred at r.t. for 1 hour. The mixture was diluted with dichloromethane and NH₄Cl, and the organic layer was washed with brine, dried (anhyd. Na₂SO₄), and concentrated. The crude material was purified by SiO₂ column chromatography (hexanes: ethyl acetate = 4: 1) to give **N, N-di-butoxycarbonyl 1-(6-hydroxyhexyl)guanidine** as a colorless oil (305 mg, quant.). ¹H-NMR (500 MHz, CDCl₃): δ ppm 11.50 (s, 1H, guanidyl), 8.30 (s, 1H, guanidyl), 3.58 (t, J = 6.6 Hz, 13.2, 2H, CH₂-O), 3.35 (m, 2H, N-CH₂), 2.00 (br, 1H, OH), 1.53 (m, 4H, CH₂, CH₂), 1.45 (d 18H, Boc), 1.34 (m, 4H, CH₂, CH₂). ¹³C-NMR (500 MHz, CDCl₃): δ ppm 163.57 156.11 153.29 104.74 83.02 79.22 62.57 60.39 40.77 32.48 28.89 28.27 28.05 26.56 25.34 21.02 14.17. HRMS (ESI): [M+Na]⁺ C₁₇H₃₃N₃O₅Na calcd for 382.2318, found 382.2312.

N, N-di-butoxycarbonyl 1-(6-hydroxyhexyl)guanidine (45 mg, 0.16 mmol) was treated with NaH (115 mg, 0.32 mmol) in THF (2 mL) at 0 °C for 5 minutes and reacted with propargylbromide (9.2 M toluene solution, 35 μ L, 0.32 mmol) at r.t. overnight. The product was extracted with ethyl acetate and sat. NH₄Cl, and the organic layer was washed with brine, dried (anhyd. Na₂SO₄), and concentrated. The residual oil was purified by SiO₂ column chromatography (hexanes: ethyl acetate = 10: 1 to 4: 1) to give the desired product as a pale yellow oil (35 mg, 75%). ¹H-NMR (500 MHz, CDCl₃): δ ppm 11.50 (s, 1H, guanidyl), 8.30 (s, 1H, guanidyl), 4.13 (d, 2H, J = 2.5 Hz, propargyl), 3.50 (t, 2H, J = 6.6 Hz, CH₂-O), 3.40 (m, 2H, N-CH₂), 1.59 (m, 4H, CH₂), 1.50 (s, 9H, Boc), 1.49 (s, 9H, Boc), 1.38 (m, 4H, CH₂). ¹³C-NMR (500 MHz, CDCl₃): δ ppm 163.62 156.11 153.34 83.05 80.00 79.28 74.16 70.02 68.00 58.06 40.91 29.34 28.95 28.32 28.10 26.65 25.79 25.63.

tert-Butyl (6-(prop-2-yn-1-yloxy)hexyl)carbamate (9b): A solution of 6-amino-1-hexanol (3.76 g, 32.1 mmol) and Boc₂O (6.3 g, 28.9 mmol) in 1,4-dioxane (30 mL) and 5N NaOH (20 mL) was stirred at r.t. overnight. The mixture was diluted with ethyl acetate and sat. KHSO₄, and the organic layer was washed with H₂O and brine, dried (anhyd. Na₂SO₄), and concentrated to give *tert*-butyl (6-hydroxyhexyl)carbamate as a colorless solid (5.27 g, 84%). HRMS (ESI): [M+Na]⁺ C₁₁H₂₃NO₃Na calcd for 240.1576, found 240.1563.

The resulting alcohol (50 mg, 0.23 mmol) was further reacted with propargyl bromide (9.2 M toluene solution, 200 μ L, 1.84 mmol) in the presence of NaH (18 mg, 0.46 mmol) THF at r.t. overnight. The reaction was diluted with ethyl acetate and sat. NH₄Cl, and the organic layer was washed with brine, dried (anhyd. Na₂SO₄), and concentrated. The residual oil was further purified by SiO₂ column chromatography (hexanes: ethyl acetate = 10: 1 to 4: 1) to afford the product as a pale yellow oil (43 mg, 73%). ¹H-NMR (500 MHz, CDCl₃): δ ppm 4.55 (s, 1H, NH), 4.13 (d, J = 2.2 Hz, 2H, O-CH₂-alkyne), 3.51 (t, 2H, O-CH₂-CH₂), 3.12 (q, 2H, NH-CH₂-), 2.43 (t, 1H, alkyne), 1.60 (m, 2H, CH₂), 1.51-1.31 (m, 15H, CH₂ and Boc). HRMS (ESI): [M+Na]⁺ C₁₄H₂₅NO₃Na calcd for 278.1732, found 278.1722.

tert-Butyl (4-(((6-(prop-2-yn-1-yloxy)hexyl)carbamoyl)phenyl)carbamate (9c): Compound **9b** (40 mg, 0.16 mmol) was treated with 25% TFA in dichloromethane at 0 °C for 30 minutes and the mixture was concentrated. To the solution of the resulting TFA salt and triethylamine (78 μ L 0.56 mmol) in dichloromethane (5 mL) was added *N*-Boc-4-amino benzoic acid (41 mg, 0.17 mmol), PyBOP (135 mg, 0.26 mmol), and HOBt (40 mg, 0.26 mmol), and the mixture was stirred at r.t. overnight. The mixture was diluted with dichloromethane, and the organic layer was washed with sat. NH₄Cl, sat. NaHCO₃, and brine, dried (anhyd. Na₂SO₄), and then concentrated. The residue was purified by SiO₂ column chromatography (hexanes: ethyl acetate = 4: 1) to afford the desired product as a colorless solid (58 mg 92%). ¹H-NMR (400 MHz, CDCl₃): δ ppm 7.70 (d, 2H, J = 8.8 Hz, aryl), 7.42 (d, 2H, J = 8.8 Hz, aryl), 6.65 (s, 1H, NH), 6.06 (t, 1H, J = 5.0 Hz, NHCO), 4.12 (d, 2H, J = 2.3 Hz, CH₂-alkyne), 3.53-3.41 (m, 4H, O-CH₂-CH₂ and NH-CH₂-CH₂), 2.40 (q, 1H, J = 2.4 Hz, alkyne), 1.68-1.58 (m, 4H, O-CH₂-CH₂ and NH-CH₂-CH₂), 1.52 (s, 9H, Boc), 1.41 (m, 4H, CH₂). ¹³C-NMR (100 MHz, CDCl₃): δ ppm 167.0, 152.5, 141.4, 129.1, 128.1, 117.9, 81.2, 80.1, 74.2, 70.2, 58.2, 40.1, 29.8, 29.5, 28.4, 26.9, 26.0. HRMS (ESI): [M+Na]⁺ C₂₁H₃₀N₂O₄Na calcd for 397.2104, found 397.2094.

N, N-di-tert-Butoxycarbonyl-4-guanidino-N-(6-(prop-2-yn-1-yloxy)hexyl)benzamide (9d): A solution of 4-aminobenzoic acid (170 mg, 1.24 mmol), (Boc)₂-1H-pyrazole-1-carboximidamide (500 mg, 1.61 mmol), and triethylamine (515 μ L, 3.72 mmol) in dichloromethane (5 mL) was stirred at r.t. overnight. The reaction mixture was diluted with ethyl acetate, and the organic layer was washed with NH₄Cl and brine, dried (anhyd. Na₂SO₄), and concentrated. The crude material was further purified by SiO₂ column chromatography (hexanes: ethyl acetate = 5: 1) to give (Z)-4-(2,3-bis(*tert*-butoxycarbonyl)guanidino)benzoic acid (**10**) as a white solid (103 mg, 22%). ¹H-NMR (400 MHz, CDCl₃): δ ppm 11.63 (s, 1H, guanidyl), 10.63 (s, 1H, guanidyl), 8.08 (d, 2H, J = 8.8 Hz, aryl), 7.78 (d, 2H, J = 8.8 Hz, aryl), 1.56 (s, 18H, Boc). HRMS (ESI): [M+Na]⁺ C₁₈H₂₅N₃O₆Na calcd for 402.1641, found 402.1629.

Compound **9b** (20 mg, 78.3 μ mol) was deprotected by treatment with 25% TFA in dichloromethane and concentrated. To a solution of the resulting free amine, triethylamine (78 μ L, 12.9 mmol), and (**10** (33 mg, 86.2 μ mol) were added PyBOP (67 mg 12.9 μ mol), HOBt (20 mg, 12.9 μ mol) in dichloromethane (2 mL), and the mixture was stirred at r.t. overnight. The solution was diluted with dichloromethane, and the organic layer was washed with sat. NH₄Cl, sat. NaHCO₃, and brine, and dried (anhyd. Na₂SO₄), and concentrated. The crude material was further purified by SiO₂ column chromatography (hexanes: ethyl acetate = 4: 1) to afford the product as a white solid (31 mg, 77%). ¹H-NMR (400 MHz, CDCl₃): δ ppm 7.70 (q, 4H, J = 8.8 Hz, aryl), 6.15 (t, 1H, J = 5.5 Hz, NHCO), 4.12 (d, 2H, J = 2.5 Hz, O-CH₂-alkyne), 3.51 (t, 2H, J = 6.5 Hz, NH-CH₂-CH₂), 3.41 (q, 2H, J = 6.7 Hz, O-CH₂-CH₂), 2.42 (t, 1H, J = 2.5 Hz, alkyne), 1.64-1.57 (m, 4H, -CH₂-), 1.52 (m, 18H, Boc), 1.46-1.35 (m, 4H, -CH₂-). ¹³C-NMR (100 MHz, CDCl₃):

δ ppm 167.0, 163.4, 153.5, 153.4, 139.8, 130.8, 127.8, 121.7, 84.2, 80.1, 80.1, 77.5, 77.4, 77.2, 76.8, 74.3, 70.2, 58.2, 40.1, 29.7, 29.5, 28.2, 26.9, 26.0, 1.2. HRMS (ESI): $[M+Na]^+$ $C_{27}H_{40}N_4O_6Na$ calcd for 539.2846, found 539.2835.

N, N-di-tert-Butoxycarbonyl-4-guanidino-N-(6-(prop-2-yn-1-yloxy)hexyl)benzamide (9e): This compound was prepared by a similar procedure to that described for **9d** using **11** (54 mg, 0.35 mmol) and **9b** (30 mg, 0.12 mol) to give **9e** as a colorless solid (40 mg 57%). 1H -NMR (400 MHz, $CDCl_3$): δ ppm 7.89 (d, 2H, J = 8.0 Hz, aryl), 7.81 (d, 2H, J = 8.0 Hz, aryl), 6.20 (s, 1H, NHCO), 4.12 (s, 2H, O-CH₂-alkyne), 3.53–3.44 (m, 4H, O-CH₂-CH₂ and NH-CH₂-CH₂), 2.40 (t, 1H, J = 2.3 Hz, alkyne), 1.66–1.60 (m, 6H, O-CH₂-CH₂ and NH-CH₂-CH₂), 1.54 (s, 9H, N' -Boc), 1.43 (m, 4H, -CH₂-), 1.35 (s, 18H, N -Boc). ^{13}C -NMR (100 MHz, $CDCl_3$): δ ppm 166.6, 158.3, 148.4, 138.1, 136.7, 128.5, 127.3, 84.6, 83.4, 80.1, 74.3, 70.2, 58.2, 40.3, 29.7, 29.5, 28.2, 27.8, 27.8, 26.9, 26.0. HRMS (ESI): $[M+Na]^+$ $C_{32}H_{47}N_3O_8Na$ calcd for 624.3261, found 624.3251.

4-(2,3-bis(tert-Butoxycarbonyl)guanidino)benzoic acid (10): A solution of 4-aminobenzoic acid (170 mg, 1.24 mmol), (Boc)₂-1H-pyrazole-1-carboximidamide (500 mg, 1.61 mmol), and TEA (515 μ L, 3.72 mmol) in dichloromethane (5 mL) was stirred at r.t. overnight. The reaction mixture was diluted with ethyl acetate, and the organic layer was washed with sat. NH_4Cl , brine, dried (anhyd. Na_2SO_4), and concentrated. The residual material was purified by SiO_2 column chromatography (hexane: ethyl acetate = 5: 1) to afford the desired product as a white solid (103 mg, 22%). 1H -NMR (400 MHz, $CDCl_3$): δ ppm 11.63 (s, 1H, guanidyl), 10.63 (s, 1H, guanidyl), 8.08 (d, 2H, J = 8.8 Hz, aryl), 7.78 (d, 2H, J = 8.8 Hz, aryl), 1.56 (s, 18H, Boc). HRMS (ESI): $[M+Na]^+$ $C_{18}H_{25}N_3O_6Na$ calcd for 402.1641, found 402.1629.

4-(N,N,N'-tris(tert-Butoxycarbonyl)carbamimidoyl)benzoic acid (11): A solution of 4-cyanobenzoic acid (2.14 g, 14.5 mmol) and conc. HCl (5 mL) in methanol (40 mL) was stirred at 40 °C for 24 hours. The mixture was concentrated, diluted with ethyl acetate and sat. $NaHCO_3$, and the aqueous layer was further extracted with ethyl acetate twice. The combined organic layer was washed with brine, dried, and concentrated to give the corresponding methyl ester as a white solid (2.16 g, 92%). 1H -NMR (400 MHz, $CDCl_3$): δ ppm 8.14–8.09 (d, 2H, J = 8.0 Hz, aryl), 7.74 (d, 2H, J = 8.0 Hz, aryl), 3.96 (s, 3H, -COOCH₃).

To a solution of the resulting methyl ester (500 mg, 3.10 mmol), hydroxylamine hydrochloride (647 mg 9.31 mmol) in methanol (10 mL) was added K_2CO_3 (750 mg 5.43 mmol), and the resulting mixture was stirred at 75 °C for 90 minutes. The mixture was diluted with ethyl acetate and H_2O (10 mL), and the aqueous layer was further extracted with ethyl acetate (90 mL). The combined organic layer was washed with brine, dried (anhyd. Na_2SO_4), and concentrated. The residual product was purified by SiO_2 column chromatography (hexanes: ethyl acetate = 4: 1 to 1: 1) to give methyl 4-(N-hydroxycarbamidoyl)benzoate (68 mg, 61%). 1H -NMR (400 MHz, $CDCl_3$): δ ppm 8.07 (d, 2H, J = 8.3 Hz aryl), 7.71 (d, 2H, J = 8.3 Hz aryl), 6.57 (s, 1H, $N'H$), 4.87 (s, 2H, NH-OH), 3.93 (s, 3H, -COOCH₃).

Hydrogenation of methyl 4-(N-hydroxycarbamidoyl)benzoate (368 mg, 1.9 mmol) in acetic acid (10 mL) in the presence of acetic anhydride (270 μ L, 2.83 mmol) and 10% Pd-C (37 mg) was carried out by stirring under the atmospheric pressure of hydrogen at r.t. overnight. Filtration and concentration gave methyl 4-carbamimidoylbenzoate acetate as a white solid (408 mg, 91%), which was used for the following Boc protection without further purification.

The resulting amidine derivative (466 mg, 1.96 mmol) was reacted with Boc₂O (640 mg, 2.93 mmol) in the presence of TEA

(812 μ L, 5.87 mmol) in methanol (16 mL) at 40 °C for 3 hours. The reaction mixture was diluted with ethyl acetate and sat. NH_4Cl , and the aqueous layer was further extracted with ethyl acetate (100 mL). The combined organic layer was dried (anhyd. Na_2SO_4) and concentrated. The resulting crude material was purified by SiO_2 column chromatography (hexanes: ethyl acetate = 4: 1) to give methyl 4-(N-(tert-butoxycarbonyl)carbamimidoyl)benzoate as a white solid (460 mg, 85%). 1H -NMR (400 MHz, $CDCl_3$): δ ppm 9.53 (s, 1H, NH), 7.99 (d, 2H, J = 8.3 Hz, aryl), 7.85 (d, 2H, J = 8.3 Hz, aryl), 6.73 (s, 1H, $N'H$), 3.90 (s, 3H, -COOCH₃), 1.52 (s, 9H, Boc).

A solution of the resulting mono Boc protected compound (113 mg, 0.41 mmol), Boc₂O (221 mg, 1.02 mmol), TEA (112 μ L, 0.81 mmol), and DMAP (50 mg, 0.41 mmol) in dichloromethane (5 mL) was stirred at r.t. for 30 minutes. The solution was diluted with ethyl acetate and sat. $KHSO_4$, and the organic layer was washed with H_2O , sat. $NaHCO_3$, and brine and dried (anhyd. Na_2SO_4). Evaporation of the solvent and SiO_2 column chromatography (hexanes: ethyl acetate = 9: 1 \rightarrow 4: 1) gave methyl (Z)-4-(N,N,N'-tris(tert-butoxycarbonyl)carbamimidoyl)benzoate as a colorless oil (188 mg 97%). 1H -NMR (400 MHz, $CDCl_3$): δ ppm 8.09 (d, 2H, J = 8.0 Hz, aryl), 7.89 (d, 2H, J = 8.0 Hz, aryl), 3.95 (s, 3H, -COOCH₃), 1.55 (s, 9H, N' -Boc), 1.35 (s, 18H, N -Boc). HRMS (ESI): $[M+Na]^+$ $C_{24}H_{34}N_2O_8Na$ calcd for 501.2213, found 501.2203.

The resulting fully Boc protected amidine derivative (188 mg 0.39 mmol) was further hydrolyzed using 2N KOH (1.96 mL 3.93 mmol) in methanol (10 mL) at r.t. for 2 hours. The mixture was acidified with 1N HCl, and the product was extracted with ethyl acetate. The organic layer was dried (anhyd. Na_2SO_4) and concentrated to give **11** (190 mg, quant.). 1H -NMR (400 MHz, $CDCl_3$): δ ppm 11.20 (s, 1H, -COOH), 8.17 (d, 2H, J = 8.3 Hz, aryl), 7.93 (d, 2H, J = 8.3 Hz, aryl), 1.35 (s, 18H, Boc). ^{13}C -NMR (100 MHz, $CDCl_3$): δ ppm 170.7, 158.1, 150.1, 148.3, 138.8, 132.6, 130.4, 128.3, 84.7, 83.5, 82.3, 80.7, 28.4, 28.1, 27.8. HRMS (ESI): $[M+Na]^+$ $C_{23}H_{32}N_2O_8Na$ calcd for 487.2057, found 487.2047.

1-(6-(Prop-2-yn-1-yloxy)hexyl)guanidine (12): To a solution of **9a** (7 mg, 0.02 mmol) in dichloromethane (1 mL) was added TFA (0.3 mL) dropwise at 0 °C, and the mixture was stirred at 0 °C for 2 hours under atmospheric argon gas. The mixture was concentrated to give the product as a colorless amorphous solid as a TFA salt (9 mg, quant.). 1H -NMR (400 MHz, $CDCl_3$): δ ppm 4.39 (m, 2H), 3.75 (m, 2H), 3.42 (m, 2H), 1.80–1.63 (m, 8H). ^{13}C -NMR (100 MHz, $CDCl_3$): δ ppm 155.00, 84.87, 67.12, 62.31, 41.47, 27.83, 27.81, 26.13, 25.27, 24.73.

4-Carbamidoyl-N-(6-(prop-2-yn-1-yloxy)hexyl)benzamide (13): To a solution of **9e** (3.4 mg, 0.006 mmol) in dichloromethane (0.4 mL) was added TFA (0.2 mL) dropwise at 0 °C, and the mixture was stirred at 0 °C for 1 hour under atmospheric argon gas and concentrated to give the desired product as a colorless amorphous solid (2.4 mg, quant.). 1H -NMR (400 MHz, 5% CD_3OD in $CDCl_3$): δ ppm 7.84–7.67 (m, 4H), 4.13 (s, 2H), 3.51 (m, 2H), 3.46 (m, 2H), 2.42 (s, 1H), 1.65–1.27 (m, 8H). ^{13}C -NMR (100 MHz, 5% CD_3OD in $CDCl_3$): δ ppm 166.65, 128.75, 127.97, 127.34, 80.03, 74.19, 70.15, 58.07, 40.27, 29.27, 27.91, 26.81, 25.84. HRMS (ESI): $[M+H]^+$ $C_{17}H_{24}N_3O_2$ calcd for 302.1862, found 302.1845.

Methyl ((1-((1-(4-(4-(10-((tert-butoxycarbonyl)amino)-14,14-dimethyl-12-oxo-2,13-dioxo-9,11-diazapentadec-10-en-1-yl)-1H-1,2,3-triazol-1-yl)benzyl)-1H-imidazol-5-yl)methyl)-4-phenylpiperidin-4-yl)carbamoyl)-L-methioninate (14a): A solution of **2** (116 mg, 0.2 mmol), **9a** (80 mg 0.2 mmol), THPTA (175 mg, 0.40 mmol), ascorbic acid (89 mg, 0.5 mmol), and $CuSO_4$ (64 mg, 0.40 mmol) in a mixture of THF (3 mL) and H_2O (3 mL) was stirred at r.t. for 15 minutes. The reaction mixture was diluted with dichloromethane

(800 mL) and sat. NH_4Cl (20 mL), and the organic layer was further washed with sat. NaHCO_3 , brine, and dried (anhyd. Na_2SO_4). Evaporation of the solvent afforded **14a** as a pale green amorphous solid (196 mg, quant.). $^1\text{H-NMR}$ (500 MHz, CDCl_3): δ ppm 11.50 (s, 1H, guanidyl), 8.30 (s, 1H, guanidyl), 7.90 (s, 1H, triazole), 7.70 (d, 3H, J = 8.5 Hz, aryl), 7.40 (d, 2H, J = 7.2 Hz, aryl), 7.28 (m, 6H, aryl), 5.33 (m, 3H, urea and benzyl), 4.68 (s, 2H, imidazole- CH_2 -piperidine), 4.42 (m, 1H, Met- α), 4.12 (m, 2H, O- CH_2 -triazole), 3.66 (s, 3H, Met-COOCH₃), 3.56 (t, 2H, J = 6.8 Hz, CH_2 -O), 3.39 (m, 4H, piperidine and N- CH_2), 2.59 (m, 2H, piperidine), 2.22 (m, 4H, piperidine), 2.03 (m, 5H, CH_2 -S- CH_3), 1.80 (m, 2H, Met(α)- CH_2), 1.49 (m, 26H, CH_2 - CH_2 - CH_2 - CH_2 , and Boc). $^{13}\text{C-NMR}$ (500 MHz, CDCl_3): δ ppm 173.25 171.19 163.64 156.21 156.12 153.34 149.74 146.42 145.84 137.76 136.58 132.44 130.91 128.77 128.06 127.28 125.29 120.94 120.55 83.07 80.00 79.27 74.16 70.94 70.02 68.53 64.33 60.42 58.05 55.11 53.46 52.32 52.11 49.00 40.87 38.61 37.03 35.52 32.04 30.36 29.67 29.54 29.34 28.95 28.32 28.10 26.72 26.65 25.85 25.78 23.74 22.97 22.67 22.21 21.10 15.45 14.22 14.15 10.98.

Methyl ((1-((1-(4-(4-(((6-(tert-butoxycarbonyl)amino)hexyl)oxy)methyl)-1H-1,2,3-triazol-1-yl)benzyl)-1H-imidazol-5-yl)methyl)-4-phenylpiperidin-4-yl)carbamoyl)-L-methioninate (14b): This compound was prepared by a similar procedure described for **14a** using **2** (50 mg, 0.09 mmol) and **9b** (22 mg 0.09 mmol); pale green amorphous solid (76 mg, quant.). $^1\text{H-NMR}$ (400 MHz, CDCl_3): δ ppm 7.88 (s, 1H, imidazole), 7.69 (s, 3H, aryl, and imidazole), 7.52 (s, 1H, triazole), 7.36-7.29 (m, 4H, aryl), 7.23 (s, 3H, J = 6.5 Hz, aryl), 5.32 (m, 3H, urea and - CH_2 -O- CH_2 -triazole), 4.98 (s, 2H, NH- CH_2 - CH_2), 4.51-4.43 (m, 2H, NH, and Met- α), 3.66 (s, 4H, s, 3H, Met-COOCH₃), 3.56 (t, 2H, J = 6.4 Hz, O- CH_2 - CH_2), 3.09 (m, 2H, NH- CH_2 - CH_2), 2.60 (s, 2H, piperidine), 2.29-2.15 (m, 6H, piperidine, and - CH_2 -), 2.09-1.96 (m, 5H, - CH_2 - CH_2 -S- CH_3), 1.77-1.60 (m, 4H, - CH_2 -), 1.45-1.25 (m, 12H, Boc, and piperidine and - CH_2 - CH_2 -S- CH_3), 0.92 (m, 1H, - CH_2 - CH_2 -S- CH_3). $^{13}\text{C-NMR}$ (100 MHz, CDCl_3): δ ppm 173.2, 156.2, 146.5, 136.6, 130.9, 128.8, 128.1, 127.3, 125.3, 120.9, 120.5, 70.9, 68.2, 64.3, 55.1, 52.3, 52.1, 49.1, 38.8, 32.1, 30.4, 30.0, 29.7, 29.6, 28.9, 28.4, 26.6, 25.8, 23.8, 23.0, 15.4, 14.1, 11.0. HRMS (ESI): $[\text{M}+\text{Na}]^+$ $\text{C}_{43}\text{H}_{61}\text{N}_9\text{O}_6\text{SNa}$ calcd for 854.4364, found 854.4366.

Methyl ((1-((1-(4-(4-(((6-(tert-butoxycarbonyl)amino)benzamido)hexyl)oxy)methyl)-1H-1,2,3-triazol-1-yl)benzyl)-1H-imidazol-5-yl)methyl)-4-phenylpiperidin-4-yl)carbamoyl)-L-methioninate (14c): This compound was prepared by a similar procedure described for **14a** using **2** (31 mg, 0.05 mmol) and **9c** (20 mg 0.05 mmol). The residue material was purified by SiO_2 column chromatography (chloroform: Acetone: EtOH = 100: 40: 8) to give **14c** as a colorless amorphous solid (29 mg, 58%). $^1\text{H-NMR}$ (400 MHz, CDCl_3): δ ppm 7.90 (s, 1H, NH), 7.70-7.68 (m, 7H, aryl), 7.53 (dd, 2H, J = 5.6, 3.4 Hz, aryl), 7.42 (s, 3H, aryl, and imidazole), 7.32 (s, 1H, aryl), 7.21 (d, 2H, aryl), 6.90 (s, 1H, imidazole), 6.20 (s, 1H, NHCO), 5.22 (m, 2H, NH, and urea), 4.67 (s, 2H, benzyl), 4.42 (d, 1H, J = 4.5 Hz, Met- α), 4.31-4.26 (m, 4H, NH- CH_2 - CH_2 , and - CH_2 -O- CH_2 -triazole), 3.65 (s, 3H, s, 3H, Met-COOCH₃), 3.56 (t, 2H, J = 6.1 Hz, O- CH_2 - CH_2), 3.42 (t, 3H, J = 6.3 Hz, NH- CH_2 - CH_2), 2.54 (s, 2H, piperidine), 2.25 (s, 4H, piperidine), 2.04-1.99 (m, 5H, - CH_2 - CH_2 -S- CH_3), 1.74 (dd, 2H, J = 13.1, 7.1 Hz, piperidine), 1.65-1.58 (m, 4H, - CH_2 -), 1.52 (s, 9H, Boc), 1.45-1.39 (m, 2H, - CH_2 -), 1.32 (s, 1H, - CH_2 - CH_2 -S- CH_3), 0.94-0.88 (m, 1H, - CH_2 - CH_2 -S- CH_3). $^{13}\text{C-NMR}$ (100 MHz, CDCl_3): δ ppm 166.9, 152.4, 141.4, 131.0, 130.9, 128.8, 128.7, 127.9, 125.2, 120.9, 120.6, 117.8, 81.0, 77.7, 70.8, 68.2, 64.3, 55.2, 52.3, 52.1, 39.9, 38.8, 32.1, 30.4, 29.7, 29.6, 29.5, 28.9, 28.5, 28.3, 26.7, 25.8, 23.8, 23.0, 15.4, 14.1, 14.1, 11.0, 1.0. HRMS (ESI): $[\text{M}+\text{Na}]^+$ $\text{C}_{50}\text{H}_{66}\text{N}_{10}\text{O}_7\text{SNa}$ calcd for 973.4735, found 973.4738.

Methyl ((1-((1-(4-(4-(((6-(2,3-bis(tert-butoxycarbonyl)guanidino)benzamido)hexyl)oxy)methyl)-1H-1,2,3-triazol-1-yl)benzyl)-

1H-imidazol-5-yl)methyl)-4-phenylpiperidin-4-yl)carbamoyl)-L-methioninate (14d): This compound was prepared by a similar procedure described for **14a** using **2** (22 mg, 0.04 mmol) and **9d** (20 mg 0.04 mmol). The residual product was purified by SiO_2 column chromatography (chloroform: acetone: EtOH = 100: 40: 8) to give **14d** as a colorless amorphous solid (33 mg, 79%). $^1\text{H-NMR}$ (400 MHz, CDCl_3): δ ppm 11.62 (s, 1H, guanidyl), 10.50 (s, 1H, guanidyl), 7.91 (s, 1H, imidazole), 7.74-7.70 (m, 5H, aryl), 7.39 (m, 2H, aryl), 7.29 (d, 2H, J = 9.5 Hz, aryl), 7.21 (d, 1H, J = 6.5 Hz, aryl), 7.08 (s, 1H, imidazole), 6.97 (d, 2H, J = 7.0 Hz, aryl), 6.33 (s, 1H, NHCO), 5.55-5.23 (m, 3H, - CH_2 -O- CH_2 -triazole, and urea), 4.69 (s, 2H, benzyl), 4.44 (d, 1H, J = 5.3 Hz, Met- α), 3.66 (s, 3H, Met-COOCH₃), 3.57 (t, 2H, J = 6.0 Hz, NH- CH_2 - CH_2), 3.49-3.38 (m, 4H, N- CH_2 -imidazole, and O- CH_2 - CH_2), 2.56 (s, 2H, piperidine), 2.29 (m, 4H, piperidine), 2.18-2.05 (m, 4H, O- CH_2 - CH_2 , and NH- CH_2 - CH_2), 2.00 (m, 5H, - CH_2 - CH_2 -S- CH_3), 1.83-1.74 (m, 2H, - CH_2 -), 1.61 (q, 2H, J = 6.4 Hz, - CH_2 -), 1.55 (s, 9H, Boc), 1.51 (s, 9H, Boc), 1.39 (m, 2H, piperidine), 1.26-1.16 (m, 1H, - CH_2 - CH_2 -S- CH_3), 0.89 (s, 1H, - CH_2 - CH_2 -S- CH_3). $^{13}\text{C-NMR}$ (100 MHz, CDCl_3): δ ppm 173.4, 167.0, 163.3, 156.5, 153.4, 153.3, 146.4, 139.7, 136.5, 130.5, 128.6, 128.1, 127.7, 127.0, 125.2, 121.6, 120.9, 120.7, 119.4, 84.1, 80.0, 70.8, 64.3, 55.2, 52.2, 52.1, 49.1, 40.0, 36.8, 35.7, 32.2, 29.8, 29.6, 29.5, 28.2, 28.1, 26.8, 25.8, 15.4. HRMS (ESI): $[\text{M}+\text{Na}]^+$ $\text{C}_{56}\text{H}_{76}\text{N}_{12}\text{O}_9\text{SNa}$ calcd for 1115.5477, found 1115.5487.

Methyl ((4-phenyl-1-((1-(4-(4-(((6-(4-(N,N,N'-tris(tert-butoxycarbonyl)carbamimidoyl)benzamido)hexyl)oxy)methyl)-1H-1,2,3-triazol-1-yl)benzyl)-1H-imidazol-5-yl)methyl)piperidin-4-yl)carbamoyl)-L-methioninate (14e): This compound was prepared by a similar procedure described for **14a** using **2** (25 mg, 0.04 mmol) and **9e** (26 mg 0.04 mmol). The residual solid was purified by SCX column (methanol to 0.2 M NH_3 /methanol) to give **14e** as a colorless amorphous solid (46 mg, 90%). $^1\text{H-NMR}$ (400 MHz, CDCl_3): δ ppm 7.90-7.80 (m, 4H, aryl), 7.70 (d, 2H, J = 8.3 Hz, aryl), 7.60 (s, 1H, imidazole), 7.38 (d, 2H, J = 7.5 Hz, aryl), 7.32 (t, 1H, J = 7.4 Hz, aryl), 7.23 (d, 2H, J = 7.0 Hz, aryl), 6.98 (s, 1H, imidazole), 6.28 (t, 1H, J = 5.3 Hz, NHCO), 5.32 (s, 2H, benzyl), 4.82 (d, 2H, urea), 4.68 (s, 2H, N- CH_2 -imidazole), 4.43 (q, 1H, J = 7.6 Hz, Met- α), 3.66 (s, 3H, Met-COOCH₃), 3.58 (t, 2H, J = 6.4 Hz, O- CH_2 - CH_2), 3.46 (q, 2H, J = 6.6 Hz, NH- CH_2 - CH_2), 3.37 (s, 2H, piperidine), 2.62 (s, 2H, piperidine), 2.30 (t, 1H, J = 12.0 Hz, O- CH_2 - CH_2), 2.23-2.14 (m, 2H, NH- CH_2 - CH_2), 1.99-1.94 (m, 4H, - CH_2 -O- CH_2 -triazole, - CH_2 - CH_2 -S- CH_3), 1.54 (s, 9H, N'-Boc), 1.44 (s, 4H, - CH_2 -), 1.39 (s, 2H, piperidine), 1.36 (s, 18H, N-Boc), 1.25 (m, 3H, piperidine, and - CH_2 - CH_2 -S- CH_3), 0.88 (m, 1H, - CH_2 - CH_2 -S- CH_3). $^{13}\text{C-NMR}$ (100 MHz, CDCl_3): δ ppm 173.4, 166.5, 158.1, 156.5, 148.3, 146.3, 138.0, 136.5, 136.4, 128.6, 128.3, 127.3, 127.0, 125.2, 120.9, 120.7, 84.5, 83.3, 70.8, 64.2, 55.2, 52.2, 52.1, 49.2, 40.2, 36.7, 35.8, 32.2, 29.8, 29.5, 28.0, 27.7, 26.8, 25.8, 15.4. HRMS (ESI): $[\text{M}+\text{Na}]^+$ $\text{C}_{61}\text{H}_{83}\text{N}_{11}\text{O}_{11}\text{SNa}$ calcd for 1200.5892, found 1200.5902.

Methyl ((1-((1-(4-(4-(((6-guanidino)hexyl)oxy)methyl)-1H-1,2,3-triazol-1-yl)benzyl)-1H-imidazol-5-yl)methyl)-4-phenylpiperidin-4-yl)carbamoyl)-L-methioninate (4a): To a solution of **14a** (196 mg, 0.20 mmol) in dichloromethane (3 mL) was added TFA (1 mL) at 0 °C. The mixture was stirred at 0 °C for 6 hours and concentrated to give **4a** as a yellow amorphous solid (253 mg, quant.). $^1\text{H-NMR}$ (500 MHz, $\text{DMSO}-d_6$) δ ppm 9.73 (s, 1H, guanidyl), 8.78 (d, 1H, J = 19.8 Hz, guanidyl), 7.96 (d, 2H, J = 7.3 Hz, aryl), 7.67 (s, 1H, imidazole), 7.46 (d, 2H, J = 6.5 Hz, aryl), 7.30-7.17 (m, 5H, aryl), 7.05 (s, 1H, imidazole), 6.56 (s, 1H, urea), 5.60 (s, 2H, guanidyl- CH_2 - CH_2), 4.61 (d, 2H, J = 21.5 Hz, N- CH_2 -imidazole), 4.16 (d, 1H, J = 6.3 Hz, Met- α), 3.63-3.61 (m, 7H, piperidine, and Met-COOCH₃ and benzyl), 3.51-3.48 (m, 2H, O- CH_2 - CH_2), 3.08 (m, 2H, piperidine), 2.54 (s, 2H, piperidine), 2.15-2.41 (m, 2H, - CH_2 - CH_2 -S- CH_3), 2.05 (s, 3H, - CH_2 - CH_2 -S- CH_3), 1.96-1.80 (m, 2H, guanidyl- CH_2 - CH_2), 1.53 (m, 2H, - CH_2 -), 1.46 (m, 2H, - CH_2 -), 1.27

(m, 5H, piperidine, and $-\text{CH}_2-$ and $-\text{CH}_2-\text{CH}_2-\text{SCH}_3$), 0.89–0.85 (m, 1H, $-\text{CH}_2-\text{CH}_2-\text{SCH}_3$). ^{13}C -NMR (100 MHz, $\text{DMSO}-d_6$): δ ppm 173.6, 158.7, 158.4, 158.2, 157.4, 157.3, 157.2, 145.9, 136.8, 136.5, 136.4, 132.1, 129.3, 129.1, 128.5, 128.4, 126.8, 125.8, 125.3, 124.9, 124.7, 122.5, 122.4, 120.7, 120.6, 81.0, 77.3, 72.7, 70.2, 70.2, 70.0, 69.6, 68.0, 65.7, 63.6, 61.7, 60.7, 57.8, 56.0, 54.6, 52.3, 52.2, 52.1, 51.9, 49.3, 49.0, 48.5, 32.0, 31.9, 29.9, 29.8, 29.5, 29.3, 28.9, 26.4, 26.3, 25.7, 15.1. HRMS(ESI): $[\text{M}+\text{H}]^+$ calcd. for $\text{C}_{39}\text{H}_{56}\text{N}_{11}\text{O}_4\text{S}$: 774.4232; found: 774.4233.

Methyl ((1-((1-(4-(((6-aminohexyl)oxy)methyl)-1H-1,2,3-triazol-1-yl)benzyl)-1H-imidazol-5-yl)methyl)-4-phenylpiperidin-4-yl)carbamoyl)-L-methioninate (4b): To a solution of **14b** (72 mg, 0.09 mmol) in dichloromethane (4 mL) was added TFA (1 mL) at 0 °C. The solution was stirred at 0 °C for 2 hours and concentrated to give **4b** as a yellow amorphous solid (110 mg, quant.). ^1H -NMR (400 MHz, $\text{DMSO}-d_6$): δ ppm 8.83 (s, 1H, NH_2), 7.96 (s, 3H, aryl, and imidazole), 7.24 (m, 4H, aryl), 6.96 (s, 1H, imidazole), 5.75 (s, 1H, urea), 4.57 (s, 2H, benzyl), 4.15–4.08 (m, 3H, $-\text{CH}_2-\text{O}-\text{CH}_2-$ triazole, and Met- α), 3.59 (s, 4H, N- CH_2 -imidazole, and O- CH_2-CH_2), 3.47 (t, 2H, $J = 6.0$ Hz, $\text{NH}-\text{CH}_2-\text{CH}_2$), 3.43–3.38 (m, 2H, $-\text{CH}_2-$), 2.75 (s, 2H, piperidine), 2.50 (m, 2H, piperidine), 2.32 (m, 2H, piperidine, and $\text{NH}-\text{CH}_2-\text{CH}_2$), 2.02 (s, 3H, Met-COOCH₃), 1.93–1.77 (m, 2H, $-\text{CH}_2-$), 1.52 (d, 4H, $J = 4.0$ Hz, $-\text{CH}_2-\text{CH}_2-\text{SCH}_3$, and piperidine), 1.30 (m, 4H, $-\text{CH}_2-\text{CH}_2-\text{SCH}_3$, and $-\text{CH}_2-\text{CH}_2-\text{SCH}_3$), 0.83 (m, 1H, $-\text{CH}_2-\text{CH}_2-\text{SCH}_3$). ^{13}C -NMR (100 MHz, CDCl_3): δ ppm 173.7, 159.5, 159.2, 157.8, 145.8, 137.0, 129.8, 128.5, 125.4, 122.6, 120.8, 77.3, 70.0, 69.4, 63.6, 57.7, 54.5, 52.2, 52.0, 48.4, 31.8, 29.9, 29.3, 29.1, 27.3, 26.1, 26.0, 25.6, 15.0. HRMS(ESI): $[\text{M}+\text{Na}]^+$ $\text{C}_{38}\text{H}_{53}\text{N}_9\text{O}_4\text{SNa}$ calcd for 754.3839, found 754.3838.

Methyl ((1-((1-(4-(((6-(4-aminobenzamido)hexyl)oxy)methyl)-1H-1,2,3-triazol-1-yl)benzyl)-1H-imidazol-5-yl)methyl)-4-phenylpiperidin-4-yl)carbamoyl)-L-methioninate (4c): To a solution of **14c** (29 mg, 0.03 mmol) in dichloromethane (3 mL) was added TFA (1 mL) at 0 °C. The solution was stirred at 0 °C for 2 hours and concentrated to give **4c** as a pale amorphous solid (34 mg, 94%). ^1H -NMR (500 MHz, $\text{DMSO}-d_6$): δ ppm 8.82 (s, 1H), 7.97 (s, 2H), 7.73–7.66 (m, 1H), 7.56 (d, 1H, $J = 8.2$ Hz), 7.49 (d, 1H, $J = 6.7$ Hz), 7.34–7.20 (m, 3H), 6.61–6.91 (1H), 6.56–6.51 (m, 2H), 5.62 (s, 1H), 4.58 (s, 2H), 4.23–4.13 (m, 1H), 3.63 (d, 2H, $J = 11.6$ Hz), 3.51–3.48 (m, 2H), 3.19–3.16 (m, 2H), 2.55 (s, 2H), 2.47 (d, 1H, $J = 7.6$ Hz), 2.02 (s, 2H), 1.95–1.89 (m, 1H), 1.85–1.78 (m, 1H), 1.63 (s, 1H), 1.53 (q, 1H, $J = 6.6$ Hz), 1.47 (q, 1H, $J = 6.6$ Hz), 1.33–1.29 (m, 3H), 1.24 (s, 1H), 0.89–0.84 (m, 1H). ^{13}C -NMR (125 MHz, $\text{DMSO}-d_6$): δ ppm 177.3, 173.6, 166.5, 162.8, 159.4, 156.7, 152.6, 151.3, 151.2, 147.2, 145.9, 139.4, 138.7, 136.9, 136.1, 132.2, 132.0, 129.7, 129.5, 129.1, 128.6, 125.3, 122.9, 122.5, 121.1, 120.8, 113.4, 101.0, 100.8, 94.0, 91.4, 87.5, 78.7, 74.4, 70.2, 63.7, 54.5, 53.2, 52.3, 51.9, 48.6, 47.9, 45.0, 41.6, 41.3, 40.9, 39.4, 38.6, 32.0, 30.3, 29.8, 29.6, 28.8, 26.8, 25.9, 23.7, 15.1, 14.4, 13.8, 11.3. HRMS(ESI): $[\text{M}+\text{Na}]^+$ $\text{C}_{45}\text{H}_{58}\text{N}_{10}\text{O}_5\text{SNa}$ calcd for 873.4210, found 873.4214.

Methyl ((1-((1-(4-(((6-(4-guanidinobenzamido)hexyl)oxy)methyl)-1H-1,2,3-triazol-1-yl)benzyl)-1H-imidazol-5-yl)methyl)-4-phenylpiperidin-4-yl)carbamoyl)-L-methioninate (4d): To a solution of **14d** (8 mg, 0.007 mmol) in dichloromethane (0.5 mL) was added TFA (0.5 mL) at 0 °C. The solution was stirred at 0 °C for 6 hours and concentrated to give **4d** as a pale yellow amorphous solid (11 mg, quant.). ^1H -NMR (500 MHz, $\text{DMSO}-d_6$): δ ppm 10.02 (s, 1H), 8.81 (s, 1H), 8.47 (t, 1H, $J = 5.2$ Hz), 7.96 (d, 2H, $J = 8.2$ Hz), 7.90 (d, 2H, $J = 8.2$ Hz), 7.62 (s, 5H), 7.46 (d, 2H, $J = 8.2$ Hz), 7.30–7.23 (m, 6H), 6.45 (s, 1H), 6.21 (dd, 1H, $J = 12.7$, 5.3 Hz), 5.57 (s, 2H), 5.43 (s, 1H), 4.79 (d, 1H, $J = 3.4$ Hz), 4.58 (s, 2H), 4.17 (dd, 1H, $J = 12.2$, 7.6 Hz), 3.61 (s, 3H), 3.24 (s, 5H), 3.17 (s, 7H), 2.00–2.07 (3H), 1.48–1.60 (5H), 1.27–1.40 (5H), 1.14–1.28 (3H), 0.95–1.09 (4H), 0.79–0.89 (2H). ^{13}C -NMR (125 MHz, $\text{DMSO}-d_6$): δ ppm 197.6, 197.3, 173.7, 165.6, 158.7, 156.1, 149.7, 148.0,

146.9, 145.9, 145.3, 143.1, 139.5, 138.6, 136.7, 132.4, 130.8, 129.6, 129.2, 129.1, 128.7, 128.6, 128.6, 128.0, 126.8, 125.5, 125.2, 123.7, 122.5, 120.7, 116.8, 102.0, 97.5, 79.1, 75.9, 75.5, 73.4, 73.1, 72.3, 70.2, 69.8, 66.2, 63.6, 60.7, 60.0, 58.5, 52.3, 51.9, 49.1, 48.6, 47.1, 42.3, 41.5, 41.3, 41.0, 40.8, 40.6, 40.4, 40.2, 40.1, 36.2, 32.0, 29.8, 29.6, 29.4, 29.1, 27.0, 26.8, 26.7, 25.9, 23.3, 22.4, 21.8, 20.9, 15.1, 10.5. HRMS(ESI): $[\text{M}+\text{Na}]^+$ $\text{C}_{46}\text{H}_{60}\text{N}_{12}\text{O}_5\text{SNa}$ calcd for 915.4428, found 915.4427.

Methyl ((1-((1-(4-(((6-(4-carbamimidoylbenzamido)hexyl)oxy)methyl)-1H-1,2,3-triazol-1-yl)benzyl)-1H-imidazol-5-yl)methyl)-4-phenylpiperidin-4-yl)carbamoyl)-L-methioninate (4e): To a solution of **14e** (10 mg, 0.008 mmol) in dichloromethane (0.5 mL) was added TFA (0.5 mL) at 0 °C. The solution was stirred at 0 °C for 2 hours and concentrated to give **4e** as a pale amorphous solid (11 mg, quant.). ^1H -NMR (400 MHz, $\text{DMSO}-d_6$): δ ppm 12.06 (s, 1H, NH), 9.55 (s, 1H, imidazole), 9.31 (m, 2H, aryl), 8.82 (d, 1H, $J = 23.0$ Hz, imidazole), 8.14–7.93 (m, 4H, aryl), 7.67 (s, 1H, imidazole), 7.47–7.21 (m, 4H, aryl), 7.02 (s, 1H, aryl), 5.86 (s, 1H, NHCO), 4.56 (d, 2H, $J = 9.8$ Hz, benzyl), 4.15 (s, 1H, Met- α), 3.87–3.26 (m, 11H, Met-COOCH₃, and $\text{NH}-\text{CH}_2-\text{CH}_2$ and N- CH_2 -imidazole and O- CH_2-CH_2 and piperidine), 2.50 (m, 4H, piperidine), 1.96 (m, 4H, piperidine, and $-\text{CH}_2-$), 1.52 (m, 5H, $-\text{CH}_2-$, and $-\text{CH}_2-\text{CH}_2-\text{SCH}_3$), 1.32 (m, 5H, $-\text{CH}_2-$, and $-\text{CH}_2-\text{CH}_2-\text{SCH}_3$ and $-\text{CH}_2-\text{CH}_2-\text{SCH}_3$), 0.86 (s, 1H, $-\text{CH}_2-\text{CH}_2-\text{SCH}_3$). ^{13}C -NMR (100 MHz, CDCl_3): δ ppm 174.6, 173.6, 165.6, 165.2, 158.0, 146.9, 145.9, 139.5, 137.8, 137.2, 134.8, 132.2, 132.1, 130.5, 130.5, 129.5, 129.1, 128.7, 128.5, 128.0, 127.0, 125.5, 124.8, 124.0, 122.6, 121.0, 70.2, 67.9, 63.6, 54.5, 52.3, 52.0, 50.0, 48.4, 46.8, 38.9, 33.4, 33.1, 32.3, 31.9, 30.3, 29.9, 29.5, 29.5, 29.4, 28.8, 26.8, 25.9, 23.7, 22.9, 19.6, 15.1, 14.4, 14.0, 11.3. HRMS(ESI): $[\text{M}+\text{H}]^+$ $\text{C}_{46}\text{H}_{60}\text{N}_{11}\text{O}_5\text{S}$ calcd for 878.4499, found 878.4499.

((1-((1-(4-(((6-Guanidino)hexyl)oxy)methyl)-1H-1,2,3-triazol-1-yl)benzyl)-1H-imidazol-5-yl)methyl)-4-phenylpiperidin-4-yl)carbamoyl)-L-methionine (5a): To a solution of **4a** (253 mg, 0.2 mmol) in methanol (30 mL) was added 0.1 N KOH (2 mmol) dropwise at 0 °C, and the solution was stirred at 0 °C for 6 hours. After neutralization by adding 2N HCl, the reaction mixture was concentrated. The residue was passed through C18 column (10% methanol in dichloromethane to dichloromethane) to give **5a** as a pale yellow amorphous solid (70 mg, 30%). ^1H -NMR (400 MHz, $\text{DMSO}-d_6$): δ ppm 12.05 (s, 1H, guanidyl), 10.64 (s, 1H, guanidyl), 9.27 (s, 1H, guanidyl), 8.87 (s, 1H, imidazole), 8.04 (m, 6H, aryl, and imidazole), 7.66 (s, 2H, aryl), 7.39 (d, 3H, $J = 6.8$ Hz, aryl), 7.30 (t, 2H, $J = 6.8$ Hz, aryl), 7.21 (t, 1H, $J = 6.8$ Hz, aryl), 6.85 (d, 1H, $J = 6.8$ Hz, urea), 5.90 (s, 2H, piperidine), 4.58 (s, 4H, N- CH_2 -imidazole, and Met- α), 4.09 (s, 2H, O- CH_2 -triazole), 3.60–3.38 (m, 8H, piperidine, and guanidyl- CH_2-CH_2 and benzyl and O- CH_2-CH_2), 2.72–2.68 (m, 2H, piperidine), 2.04 (s, 3H, $-\text{CH}_2-\text{CH}_2-\text{SCH}_3$), 1.97–1.88 (m, 2H, $-\text{CH}_2-$), 1.84–1.76 (m, 2H, $-\text{CH}_2-$), 1.53 (s, 4H, piperidine, and $-\text{CH}_2-$), 1.27 (m, 7H, $-\text{CH}_2-$, and $-\text{CH}_2-\text{CH}_2-\text{SCH}_3$ and $-\text{CH}_2-\text{CH}_2-\text{SCH}_3$), 0.89–0.80 (m, 1H, $-\text{CH}_2-\text{CH}_2-\text{SCH}_3$). ^{13}C -NMR (100 MHz, $\text{DMSO}-d_6$): δ ppm 174.6, 158.0, 147.0, 145.9, 137.2, 135.0, 130.4, 129.2, 128.5, 126.9, 125.5, 122.6, 121.0, 81.0, 77.4, 70.0, 69.5, 63.6, 57.8, 54.5, 52.0, 48.4, 33.1, 32.9, 32.2, 30.0, 29.3, 29.2, 27.3, 26.1, 25.9, 25.6, 15.1. HRMS(ESI): $[\text{M}+\text{H}]^+$ calcd. for $\text{C}_{38}\text{H}_{54}\text{N}_{11}\text{O}_4\text{S}$: 760.4076; found: 760.4069.

((1-((1-(4-(((6-Aminohexyl)oxy)methyl)-1H-1,2,3-triazol-1-yl)benzyl)-1H-imidazol-5-yl)methyl)-4-phenylpiperidin-4-yl)carbamoyl)-L-methionine (5b): Compound **4b** (29 mg, 0.003 mmol) was hydrolyzed by a similar procedure described for **5a** to give **5b** as a pale yellow amorphous solid (19 mg, 85%). ^1H -NMR (400 MHz, $\text{DMSO}-d_6$): δ ppm 12.08 (s, 1H, NH_2), 9.24 (s, 1H, imidazole), 8.88 (s, 1H, imidazole), 8.00 (d, 2H, $J = 7.8$ Hz, aryl), 7.88 (s, 1H, imidazole), 7.67 (d, 2H, $J = 7.8$ Hz, aryl), 7.50–7.38 (m, 3H), 7.32–7.29 (m, 2H, aryl), 7.21 (t, 2H, $J = 6.8$ Hz, aryl), 7.06 (d, 1H, $J = 6.8$ Hz, aryl), 6.81 (d, 1H, J

= 7.3 Hz, urea), 5.88 (s, 2H, piperidine), 4.58 (s, 3H, N-CH₂-imidazole, and Met- α), 4.10 (s, 2H, -CH₂-O-CH₂-triazole), 3.61 (s, 2H, NH-CH₂-CH₂), 3.48 (m, 6H, piperidine, and benzyl and O-CH₂-CH₂), 3.09 (q, 2H, *J* = 6 Hz, piperidine), 2.04 (s, 3H, -CH₂-CH₂-SCH₃), 1.95-1.88 (m, 4H, -CH₂-), 1.52 (t, 2H, *J* = 6 Hz, -CH₂-), 1.47 (t, 2H, *J* = 13.3 Hz, -CH₂-), 1.31-1.23 (m, 5H, -CH₂-CH₂-SCH₃, and piperidine and -CH₂-CH₂-SCH₃), 0.89-0.84 (m, 1H, -CH₂-CH₂-SCH₃). ¹³C-NMR (100 MHz, DMSO-*d*₆): δ ppm 174.6, 158.0, 157.6, 147.0, 145.9, 137.2, 134.9, 130.4, 129.2, 128.5, 126.9, 125.5, 125.1, 122.6, 121.0, 120.8, 70.1, 63.7, 54.5, 52.2, 52.0, 50.0, 48.4, 46.8, 41.1, 37.0, 36.9, 34.5, 33.6, 32.9, 32.3, 31.9, 31.8, 31.4, 30.0, 29.9, 29.5, 28.9, 28.8, 26.3, 25.7, 22.5, 15.1, 14.4, 14.4, 11.3. HRMS (ESI): [M+Na]⁺ C₃₇H₅₁N₉O₄Na calcd for 740.3683, found 740.3682.

((1-((1-(4-(4-(((6-(4-Aminobenzamido)hexyl)oxy)methyl)-1H-1,2,3-triazol-1-yl)benzyl)-1H-imidazol-5-yl)methyl)-4-phenylpiperidin-4-yl)carbamoyl)-L-methionine (5c): Compound **4c** (20 mg, 0.02 mmol) was hydrolyzed by a similar procedure described for **5a** to give **5c** as a pale yellow amorphous solid (18 mg, 90%). ¹H-NMR (500 MHz, DMSO-*d*₆): δ ppm 12.01 (s, 1H), 9.26 (s, 1H), 8.86 (s, 1H), 8.33 (s, 1H), 8.16 (s, 1H), 8.00 (d, 2H, *J* = 8.2 Hz), 7.77-7.67 (m, 5H), 7.40-7.21 (m, 6H), 7.06 (t, 2H, *J* = 7.8 Hz), 6.74 (d, 1H, *J* = 26.2 Hz), 5.86 (s, 2H), 4.57 (d, 4H, *J* = 15.0 Hz), 4.17-4.12 (m, 1H), 3.49 (d, 4H, *J* = 13.1 Hz), 3.38 (d, 1H, *J* = 7.0 Hz), 3.21 (q, 2H, *J* = 6.1 Hz), 2.55 (s, 2H), 2.04 (s, 2H), 1.95-1.90 (m, 1H), 1.81 (td, 1H, *J* = 13.7, 7.3 Hz), 1.52 (td, 4H, *J* = 13.3, 6.6 Hz), 1.36-1.28 (m, 5H), 0.89-0.85 (m, 1H). ¹³C-NMR (125 MHz, DMSO-*d*₆): δ ppm 174.6, 174.0, 167.5, 166.0, 158.0, 157.8, 146.9, 145.9, 137.8, 137.3, 134.7, 132.2, 132.1, 130.5, 129.2, 129.1, 128.6, 128.6, 127.0, 125.5, 125.1, 124.7, 124.0, 122.6, 121.0, 119.3, 119.2, 118.8, 118.7, 70.2, 67.9, 63.6, 60.7, 54.5, 52.0, 51.8, 50.0, 49.8, 48.4, 46.7, 41.1, 40.9, 40.8, 38.5, 38.5, 38.4, 33.5, 33.0, 32.3, 31.8, 30.3, 30.0, 29.6, 29.5, 29.2, 28.8, 26.8, 25.9, 25.6, 25.5, 23.7, 22.9, 15.1, 14.9, 14.4, 11.3. HRMS (ESI): [M+H]⁺ C₄₄H₅₇N₁₀O₅S calcd for 837.4234, found 837.4235.

((1-((1-(4-(4-(((6-(4-Guanidinobenzamido)hexyl)oxy)methyl)-1H-1,2,3-triazol-1-yl)benzyl)-1H-imidazol-5-yl)methyl)-4-phenylpiperidin-4-yl)carbamoyl)-L-methionine (5d): Compound **4d** (9 mg, 0.007 mmol) was hydrolyzed by a similar procedure described for **5a** to give **5d** as a pale yellow amorphous solid (7 mg, quant.). ¹H-NMR (500 MHz, DMSO-*d*₆): δ ppm 11.96 (s, 1H), 10.34 (d, 1H, *J* = 28.1 Hz), 9.17 (s, 1H), 8.85 (s, 1H), 8.52 (t, 1H, *J* = 5.0 Hz), 8.09 (s, 1H), 7.99 (d, 2H, *J* = 7.9 Hz), 7.91 (d, 2H, *J* = 8.2 Hz), 7.69-7.65 (m, 7H), 7.42-7.38 (m, 3H), 7.29 (t, 5H, *J* = 8.5 Hz), 7.23-7.19 (m, 2H), 6.71 (d, 1H, *J* = 7.0 Hz), 5.85 (s, 2H), 5.75 (s, 3H), 4.56 (d, 4H, *J* = 21.4 Hz), 4.15-4.08 (m, 1H), 3.25 (d, 3H, *J* = 7.6 Hz), 3.17 (s, 7H), 2.04 (s, 3H), 1.95-1.90 (m, 1H), 1.86-1.78 (m, 1H), 1.53-1.44 (m, 6H), 1.34 (d, 4H, *J* = 22.6 Hz), 1.23 (s, 5H), 1.04-1.01 (m, 2H), 0.89-0.78 (m, 3H). ¹³C-NMR (125 MHz, DMSO-*d*₆): δ ppm 178.3, 176.7, 174.6, 165.6, 162.0, 158.0, 157.0, 156.3, 149.3, 148.0, 147.0, 146.0, 145.9, 145.3, 143.1, 140.3, 139.5, 138.5, 138.0, 137.2, 134.9, 132.3, 130.7, 130.6, 130.4, 129.9, 129.5, 129.2, 129.1, 128.6, 127.0, 126.8, 126.0, 125.5, 123.9, 123.8, 123.7, 123.5, 122.6, 121.0, 116.5, 102.0, 90.0, 79.1, 75.9, 75.5, 73.4, 73.1, 72.4, 70.2, 70.2, 69.8, 66.2, 63.6, 63.5, 60.7, 60.6, 60.0, 58.5, 55.4, 54.5, 52.0, 49.9, 49.1, 48.4, 47.1, 46.8, 46.8, 42.3, 41.9, 41.7, 41.6, 41.5, 41.3, 38.6, 38.5, 34.1, 33.6, 33.0, 32.3, 31.9, 31.8, 31.7, 30.0, 29.9, 29.5, 29.5, 29.3, 29.2, 29.1, 28.9, 26.9, 26.8, 26.4, 25.9, 25.5, 25.0, 23.3, 22.6, 22.4, 21.9, 20.9, 20.4, 17.8, 16.2, 15.1, 15.0, 14.4, 10.5. HRMS (ESI): [M+Na]⁺ C₄₅H₅₈N₁₂O₅Na calcd for 901.4272, found 901.4275.

((1-((1-(4-(4-(((6-(4-Carbamimidoylbenzamido)hexyl)oxy)methyl)-1H-1,2,3-triazol-1-yl)benzyl)-1H-imidazol-5-yl)methyl)-4-phenylpiperidin-4-yl)carbamoyl)-L-methionine (5e): Compound **4e** (11 mg, 0.009 mmol) was hydrolyzed by a similar procedure described for **5a**. The residual material was purified by preparative HPLC to give **5e** (2 mg, 22%). ¹H-NMR (400 MHz, DMSO-*d*₆): δ ppm 12.29-13.04 (1H), 11.80-12.13 (1H), 9.29-9.47 (2H), 8.97-9.23 (2H), 8.74-8.85 (2H),

8.62-8.72 (1H), 8.40-8.57 (1H), 8.11-8.31 (2H), 7.98-8.05 (2H), 7.90-7.97 (3H), 7.84-7.90 (4H), 7.61-7.76 (2H), 7.48-7.58 (3H), 7.27-7.42 (5H), 7.05-7.24 (6H), 6.94-7.01 (1H), 6.57-6.75 (1H), 6.13-6.41 (3H), 5.42-5.57 (3H), 5.28-5.35 (2H), 4.54-4.63 (4H), 3.95-4.30 (7H), 3.45-3.55 (6H), 1.91-2.08 (12H), 1.41-1.61 (15H), 0.78-0.96 (17H). ¹³C-NMR (125 MHz, DMSO-*d*₆): δ ppm 174.6, 174.0, 165.6, 165.2, 158.1, 157.8, 147.0, 145.9, 139.5, 137.7, 137.2, 134.7, 130.5, 128.7, 128.6, 128.5, 128.0, 127.9, 127.5, 126.9, 125.5, 125.1, 124.6, 124.0, 122.6, 121.0, 70.2, 63.6, 55.4, 54.4, 52.0, 50.0, 49.1, 48.4, 46.7, 41.3, 40.9, 38.9, 32.2, 30.0, 29.5, 29.5, 29.4, 26.8, 25.9, 19.6, 15.1, 14.0. HRMS (ESI): [M+Na]⁺ C₄₅H₅₇N₁₁O₅Na calcd for 886.4163, found 886.4166.

Biological evaluation: Unless otherwise noted, all reagents used in the biological experiments were purchased from commercial suppliers (Sigma-Aldrich, Bio-Rad, Wako Pure Chemical Industries, or Nacalai tesque). Recombinant FTase and GGTase I were expressed and purified by the procedure previously reported in literature.³⁻⁴ The fluorogenic peptide KKKKKKSK(Dans)TKCVIM was purchased from TORAY Research Center. SDS-PAGE and western blotting were carried out with miniprotean TGX precast gels (Bio-Rad, 4–20%) using a Bio-Rad Mini-Protean III electrophoresis apparatus. Enzyme inhibition assays were performed by using a 96-well black flat bottom plate (NUNC) on Spectramax M5 (Molecular Device).^[25] The human urinary bladder carcinoma T24 cells (JCRB0711) were obtained from JCRB Cell Bank.

In vitro enzyme inhibition assay: All the kinetic measurements were performed on a fluorescence microplate reader Spectramax M5 (Molecular Device) using a 96-well black flat bottom plate (NUNC) by the procedure previously reported in literature.^[20,25] Briefly, the peptide buffer solution (50 mM Tris-HCl, pH 7.5, 0.1 mM EDTA, 0.020% *n*-dodecyl- β -maltoide, 5.0 mM DTT) was used for preparation of the fluorogenic substrate stock solution. The assay buffer solution (50 mM Tris-HCl, pH 7.5, 1.2 mM MgCl₂, 12 μ M ZnCl₂, 0.023% *n*-dodecyl- β -D-maltoide, and 5 mM DTT) was used for enzyme dilution and for running the kinetic assay. Commercially purchased FPP and GGPP ammonium salt methanol solution from Sigma-Aldrich were diluted with 25 mM NH₄HCO₃ to 500 μ M and stored at -80 °C in aliquots, and further diluted to 110 μ M before use. In a well of 96-well-black plate 10 μ L of each stock solution of farnesylpyrophosphate (FPP, 100 μ M), K-Ras4B peptide (20 μ M), recombinant FTase (2 μ M), and compound were spotted on the bottom, respectively, avoiding to mix each other. To the well 160 μ L of buffer solution was then added, resulting in mixing the spotted solutions to initiate the enzyme reaction. Time-course change of the fluorescent intensity was monitored at 520 nm (ex: 340 nm) for 5 minutes. The data was analyzed by SigmaPlot 15.

Cell viability assay: Compounds were tested against MiaPaCa2 cells. Cells (1 \times 10³ cells) were seeded in a 96-well plate (final volume 100 μ L/well) and were placed in the incubator (37 °C, 5% CO₂) overnight. The following day, the cells were treated with various concentrations of compounds and incubated at 37 °C, 5% CO₂ for 72 hours prior to the trypan blue assay. The absorbance at 490 nm was then measured and recorded.

Western blot analysis: Human K-RAS G12C MiaPaCa2 pancreatic cancer cells were obtained from American Type Culture Collection (ATCC) and were cultured in Dulbecco's Modified Eagle's Medium (DMEM) supplemented with 10% heat-inactivated fetal bovine serum (FBS) (R&D Systems, USA), 1% penicillin streptomycin (Sigma, USA). The cells were treated with the compounds, washed with phosphate buffered saline (PBS), and lysed in mammalian protein extraction reagent (product no. 78 501, Thermo Fisher Scientific, Rockford, IL, USA) supplemented with protease inhibitor cocktail (product no.

A32953, Thermo Fisher Scientific) (consisting of 2-mM phenylmethylsulfonyl fluoride, 2-mM Na₃VO₄, and 6.4-mg/mL p-nitrophenylphosphate) and phosphatase inhibitor (Product no: A32963 Thermo Fisher Scientific) as described by us.^[19] Lysates were then processed for SDS-PAGE western blotting as described by us^[19] with the following antibodies: anti-HDJ-2 (Invitrogen, Product No. PIMA512748), anti-Rap1A+B (Abcam, Product No. ab187659), anti-vinculin (Cell Signaling Technology, Product No. 13 901), and anti-K-Ras (Invitrogen, Product No. 703 345).

Computational modeling: The structural minimizations throughout the study were performed by AMBER 20.^[31] The force field parameters for amino acid residues were ff19SB,^[32] ff14SB,^[33] and GAFF or GAFF2.1^[34] with the steepest descent and conjugate gradient algorithms. The complements of the hydrogen atoms which could not be observed by X-ray crystallographical analysis and the mutated residues were performed by the tleap module of AmberTools. The initial structure (PDB ID:1MZC, 1KZO, and 1TNO) was retrieved from Protein Data Bank (PDB),^[35–37] and total complex structure was optimized. When the ligand structure was modified, at first the amino acids adjacent to the ligand were optimized, and at last the total structure was optimized. When the large substituent was added to the ligand, three conformers were generated and optimized, and the most stable structure was selected as a docking structure. Optimized structures were displayed using Chimera.^[38]

Supporting Information

Supplementary data to this article can be found online at [Supporting Information](#).

Author Contributions

N.H. performed synthesis and in vitro evaluation of compounds. R.O. and K.A. performed gel shift assays for K-Ras, HDJ2, Rap1, respectively. F.S. conducted organic synthesis, N.O. conducted antiproliferation assays. T.S. characterized synthetic compounds. Y.I. performed computational modeling. S.M.S. supervised cell-based assessments. J.O. conceptualized the research, designed the molecules, supervised the synthesis, and in vitro evaluation, and wrote the manuscript with input from all the authors.

Acknowledgments

This work was funded by JSPS (21H02077, 20K21248, 18H02106 to J.O.) and Naito Foundation (J.O.), and in part by NIH grant R35 CA197731-01 (to S.M. Sebt, PhD). This work was supported by the Instrumental Center, Shinshu University and in part by Massey Cancer Center, an NCI-designated Comprehensive Cancer Center (P30CA016059). K. Yamanaka assisted organic synthesis in part. This work was performed under the Cooperative Research Program of "Network Joint Research Center for Materials and Devices (MEXT)."

Conflict of Interest

J. Ohkanda and N. Horiuchi (JP Patent 2023–023957). All the remaining authors declare no conflict of interest.

Data Availability Statement

The data that support the findings of this study are available from the corresponding author upon reasonable request.

Keywords: bivalent inhibitors · dual inhibition · farnesyltransferase · geranylgeranyltransferase · K-Ras · peptidomimetics · posttranslational lipid modification

- [1] D. K. Simanshu, D. V. Nissley, F. McCormick, *Cell* **2017**, *170*, 17.
- [2] E. Cerami, J. Gao, U. Dogrusoz, B. E. Gross, S. O. Sumer, B. A. Aksoy, A. Jacobsen, C. Byrne, M. L. Heuer, E. Larsoo, Y. Antipin, B. Reva, A. P. Goldberg, C. Sander, N. Schultz, *Cancer Discov* **2012**, *2*, 401.
- [3] S. R. Punekar, V. Velcheti, B. G. Neel, K. K. Wong, *Nat. Rev. Clin. Oncol.* **2022**, *19*, 637.
- [4] J. John, R. Sohmen, J. Feuerstein, R. Linke, A. Wittinghofer, R. S. Goody, *Biochemistry* **1990**, *29*, 6058.
- [5] T. W. Traut, *Mol. Cell. Biochem.* **1994**, *140*, 1.
- [6] L. Boike, N. J. Henning, D. K. Nomura, *Nat. Rev. Drug Discovery* **2022**, *21*, 881.
- [7] A. Singhal, B. T. Li, E. M. O'Reilly, *Nat. Med.* **2024**, *30*, 969.
- [8] M. Garrigou, B. Sauvagnat, R. Duggal, N. Boo, P. Gopal, J. M. Johnston, A. Partridge, T. Sawyer, K. Biswas, N. Boyer, *J. Med. Chem.* **2022**, *65*, 8961.
- [9] F. Yang, Y. Wen, C. Wang, Y. Zhou, Y. Zhou, Z. M. Zhang, T. Liu, X. Lu, *Eur. J. Med. Chem.* **2022**, *230*, 114088.
- [10] X. Wang, S. Allen, J. F. Blake, V. Bowcut, D. M. Briere, A. Calinisan, J. R. Dahlke, J. B. Fell, J. P. Fischer, R. J. Gunn, J. Hallin, J. Laguer, J. D. Lawson, J. Medwid, B. Newhouse, P. Nguyen, J. M. O'Leary, P. Olson, S. Pajk, L. Rahbaek, M. Rodriguez, C. R. Smith, T. P. Tang, N. C. Thomas, D. Vanderpool, G. P. Vigers, J. G. Christensen, M. A. Marx, *J. Med. Chem.* **2022**, *65*, 3123.
- [11] M. B. Ryan, R. B. Corcoran, *Nat. Rev. Clin. Oncol.* **2018**, *15*, 709.
- [12] N. Berndt, A. D. Hamilton, S. M. Sebt, *Nat. Rev. Cancer* **2011**, *11*, 775.
- [13] C. C. Palsuledesai, M. D. Distefano, *ACS Chem. Biol.* **2015**, *10*, 51.
- [14] D. B. Whyte, P. Kirschmeier, T. N. Hockenberry, I. Nunez-Oliva, L. James, J. J. Catino, W. R. Bishop, J.-K. Pai, *J. Biol. Chem.* **1997**, *272*, 14459.
- [15] C. A. Rowell, J. J. Kowalczyk, M. D. Lewis, A. M. Garcia, *J. Biol. Chem.* **1997**, *272*, 14093.
- [16] G. L. James, J. L. Goldstein, M. S. Brown, *J. Biol. Chem.* **1995**, *270*, 6221.
- [17] F. L. Zhang, P. Kirschmeier, D. Carr, L. James, R. W. Bond, L. Wang, R. Patton, W. T. Windsor, R. Syto, R. Zhang, W. R. Bishop, *J. Biol. Chem.* **1997**, *272*, 10232.
- [18] S. B. Long, P. J. Casey, L. S. Beese, *Structure* **2000**, *8*, 209.
- [19] A. Kazi, S. Xiang, H. Yang, L. Chen, P. Kennedy, M. Ayaz, S. Fletcher, C. Cummings, H. R. Lawrence, F. Beato, Y. Kang, M. P. Kim, A. Delitto, P. W. Underwood, J. B. Fleming, J. G. Trevino, A. D. Hamilton, S. M. Sebt, *Clin. Cancer Res.* **2019**, *25*, 5984.
- [20] S. Machida, N. Kato, K. Harada, J. Ohkanda, *J. Am. Chem. Soc.* **2011**, *133*, 958.
- [21] M. Tsubamoto, T. K. Le, M. Li, T. Watanabe, C. Matsumi, P. Parvatkar, H. Fujii, N. Kato, J. Sun, J. Ohkanda, *Chem. – A Eur. J.* **2019**, *25*, 13531.
- [22] S. M. Sebt, A. D. Hamilton, Eds., *Farnesyltransferase Inhibitors in Cancer Therapy*, Humana Press, **2000**.
- [23] J. Ohkanda, F. S. Buckner, J. W. Lockman, K. Yokoyama, D. Carrico, R. Eastman, K. De Luca-Fradley, W. Davies, S. L. Croft, W. C. Van Voorhis, M. H. Gelb, S. M. Sebt, A. D. Hamilton, *J. Med. Chem.* **2004**, *47*, 432.
- [24] Y. N. Imai, Y. Inoue, Y. Yamamoto, *J. Med. Chem.* **2007**, *50*, 1189.
- [25] S. Machida, M. Tsubamoto, N. Kato, K. Harada, J. Ohkanda, *Bioorg. Med. Chem.* **2013**, *21*, 4004.
- [26] J. B. Gibbs, A. Oliff, *Annu. Rev. Pharmacol. Toxicol.* **1997**, *37*, 1433.
- [27] S. M. Sebt, C. J. Der, *Nat. Rev. Cancer* **2003**, *3*, 945.

- [28] J. Sun, M. A. Blaskovich, D. Knowles, Y. Qian, J. Ohkanda, R. D. Bailey, A. D. Hamilton, S. M. Sebt, *Cancer Res.* **1999**, *59*, 4919.
- [29] J. Canon, K. Rex, A. Y. Saiki, C. Mohr, K. Cooke, D. Bagal, K. Gaida, T. Holt, C. G. Knutson, N. Koppada, B. A. Lanman, J. Werner, A. S. Rapaport, T. San Miguel, R. Ortiz, T. Osgood, J. R. Sun, X. Zhu, J. D. McCarter, L. P. Volak, B. E. Houk, M. G. Fakih, B. H. O'Neil, T. J. Price, G. S. Falchook, J. Desai, J. Kuo, R. Govindan, D. S. Hong, W. Ouyang et al., *Nature* **2019**, *575*, 217.
- [30] N. Berndt, S. M. Sebt, *Nat. Protoc.* **2011**, *6*, 1775.
- [31] D. A. Case, M. M. Aktulga, K. Belfon, I. Y. Ben-Shalom, S. R. Brozell, D. S. Certutti, *Amber* **2021**, University of California, San Francisco. n.d.
- [32] J. A. Maier, C. Martinez, K. Kasavajhala, L. Wickstrom, K. E. Hauser, C. Simmerling, *J. Chem. Theory Comput.* **2015**, *11*, 3696.
- [33] C. Tian, K. Kasavajhala, K. A. A. Belfon, L. Raguette, H. Huang, A. N. Miguels, J. Bickel, Y. Wang, J. Pincay, Q. Wu, C. Simmerling, *J. Chem. Theory Comput.* **2020**, *16*, 528.
- [34] D. A. C. Junmei Wang, R. M. Wolf, J. W. Caldwell, P. A. Kollman, *J. Comput. Chem.* **2004**, *25*, 1157.
- [35] S. J. DeSolms, T. M. Ciccarone, S. C. MacTough, A. W. Shaw, C. A. Buser, M. Ellis-Hutchings, C. Fernandes, K. A. Hamilton, H. E. Huber, N. E. Kohl, R. B. Lobell, R. G. Robinson, N. N. Tsou, E. S. Walsh, S. L. Graham, L. S. Beese, J. S. Taylor, *J. Med. Chem.* **2003**, *46*, 2973.
- [36] S. B. Long, P. J. Casey, L. S. Beese, *Nature* **2002**, *419*, 645.
- [37] T. Scott Reid, K. L. Terry, P. J. Casey, L. S. Beese, *J. Mol. Biol.* **2004**, *343*, 417.
- [38] E. F. Pettersen, T. D. Goddard, C. C. Huang, G. S. Couch, D. M. Greenblatt, E. C. Meng, T. E. Ferrin, *J. Comput. Chem.* **2004**, *25*, 1605.
- [39] Y. Cheng, W. H. Prusoff, *Biochem. Pharmacol.* **1973**, *22*, 3099.

Manuscript received: January 24, 2025

Revised manuscript received: March 30, 2025

Version of record online: April 28, 2025